Journal of Medicinal Chemistry

THE UNIVERSITY OF MEMPHIS. University Libraries

Subscriber access provided by University Libraries, University of Memphis

Article

Discovery of cytotoxic Dolastatin 10 analogs with N-terminal modifications

Andreas Maderna, Mattew Doroski, Chakrapani Subramanyam, Alexander Porte, Carolyn Leverett, Beth C Vetelino, Zecheng Cheng, Hud Risley, Kevin Parris, Jayvardhan Pandit, Alison H. Varghese, Suman Shanker, Cynthia Song, Sai Chetan K Sukuru, Kathleen A. Farley, Melissa M Wagenaar, Michael J. Shapiro, Sylvia Musto, My-Hanh Lam, Frank Loganzo, and Christopher J. O'Donnell

J. Med. Chem., **Just Accepted Manuscript** • DOI: 10.1021/jm501649k • Publication Date (Web): 28 Nov 2014

Downloaded from http://pubs.acs.org on December 3, 2014

Just Accepted

"Just Accepted" manuscripts have been peer-reviewed and accepted for publication. They are posted online prior to technical editing, formatting for publication and author proofing. The American Chemical Society provides "Just Accepted" as a free service to the research community to expedite the dissemination of scientific material as soon as possible after acceptance. "Just Accepted" manuscripts appear in full in PDF format accompanied by an HTML abstract. "Just Accepted" manuscripts have been fully peer reviewed, but should not be considered the official version of record. They are accessible to all readers and citable by the Digital Object Identifier (DOI®). "Just Accepted" is an optional service offered to authors. Therefore, the "Just Accepted" Web site may not include all articles that will be published in the journal. After a manuscript is technically edited and formatted, it will be removed from the "Just Accepted" Web site and published as an ASAP article. Note that technical editing may introduce minor changes to the manuscript text and/or graphics which could affect content, and all legal disclaimers and ethical guidelines that apply to the journal pertain. ACS cannot be held responsible for errors or consequences arising from the use of information contained in these "Just Accepted" manuscripts.

ACS Publications
High quality. High impact.

Journal of Medicinal Chemistry is published by the American Chemical Society. 1155 Sixteenth Street N.W., Washington, DC 20036

Published by American Chemical Society. Copyright © American Chemical Society. However, no copyright claim is made to original U.S. Government works, or works produced by employees of any Commonwealth realm Crown government in the course of their duties.

Discovery of cytotoxic Dolastatin 10 analogs with N-terminal modifications

Andreas Maderna [a], Matthew Doroski [a], Chakrapani Subramanyam [a], Alexander Porte [a], Carolyn Leverett [a], Beth C. Vetelino [a], Zecheng Chen [a], Hud Risley [a] , Kevin Parris [a], Jayvardhan Pandit [a], Alison Varghese [a], Suman Shanker [a], Xi Song [a], Sai Chetan K. Sukuru [a], Kathleen A. Farley [a], Melissa M. Wagenaar [a], Michael J. Shapiro [a], Sylvia Musto [b], My-Hanh Lam [b], Frank Loganzo [b], Christopher J. O'Donnell [a]*

a Pfizer Worldwide Research and Development, Worldwide Medicinal Chemistry, Oncology Eastern Point Road, Groton, CT 06340 (USA)

b Pfizer Worldwide Research and Development, Oncology Research Unit, 401 N. Middletown Road, Pearl River, NY 10965 (USA)

KEYWORDS (Dolastatin 10 analogs, N-terminal modifications, cytotoxicity, tubulin-bound co-crystal structures, auristatin binding mode, antibody drug conjugates)

ABSTRACT

Auristatins, synthetic analogs of the antineoplastic natural product Dolastatin 10, are ultra-potent cytotoxic microtubule inhibitors that are clinically used as payloads in antibody-drug conjugates (ADCs). The design and synthesis of several new auristatin analogs with N-terminal modifications that include amino acids with α,α-disubstituted carbon atoms are described, including the discovery of our lead auristatin, PF-06380101. This modification of the peptide structure is unprecedented and led to analogs with excellent potencies in tumor cell proliferation assays and differential ADME properties when compared to other synthetic auristatin analogs that are used in the preparation of ADCs. In addition, auristatin co-crystal structures with tubulin are being presented that allow for the detailed examination of their binding modes. A surprising finding is that all analyzed analogs have a *cis*-configuration at the Val-Dil amide bond in their functionally relevant tubulin bound state, whereas in solution this bond is exclusively in the *trans*-configuration. This remarkable observation shines light onto the preferred binding mode of auristatins and serves as a valuable tool for structure based drug design.

INTRODUCTION

In 1987 Pettit *et al*. described the discovery of Dolastatin 10 (**1**), a highly cytotoxic peptide that was isolated from the sea hare *Dolabella auricularia* in the Indian Ocean.[1] This remarkable discovery was the result of fifteen years of research in which a number of cytotoxic peptides were isolated from this sea creature with Dolastatin 10 (**1**) being the most potent analog in tumor cell proliferation assays. It was soon recognized that this compound was an extremely potent mitotic spindle poison and one of several compounds produced by cyanobacteria in the intestines

of *Dolabella auricularia* that were postulated to act as defense agents against predators.[2,3,4] It was demonstrated that in addition to inhibiting tubulin polymerization **1** has a strong inhibitory effect on tubulin dependent GTP hydrolysis.[2] In order to obtain sufficient quantities for structure identification and biological testing Pettit *et. al*. collected 1000 kg of wet animal material whose combined ethanol / 2-propanol extract yielded 28.7 mg of pure Dolastatin 10 after extensive purification (Figure 1).[1]

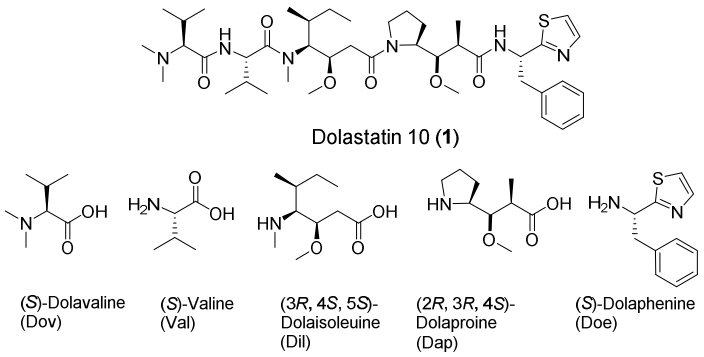

Figure 1. Structures of Dolastatin 10 (**1**) and key amino acid components.

Dolastatin 10 (**1**) is comprised of the four amino acids dolavaline (Dov), valine (Val), dolaisoleuine (Dil), dolaproine (Dap) and the C-terminal amine dolaphenine (Doe).[1,5] The binding site for **1** is located adjacent to the vinca binding site at the α,β-tubulin heterodimer interface (Figure 5).[6] Dolastatin 10 (**1**) was advanced into clinical trials, but despite encouraging preclinical efficacy data, no appreciable therapeutic index could be attained due to its significant toxicity at the maximum tolerated dose (MTD).[7-13] Shortly after the discovery of **1** a large number of synthetic analogs, termed auristatins, were prepared by Pettit *et al*., Miyazaki *et al*. and other groups with the goal to investigate the influence of structural changes on cell based potencies in tumor cell proliferation assays (Figure 2). [14-16] These efforts have been extensively reviewed.[17]

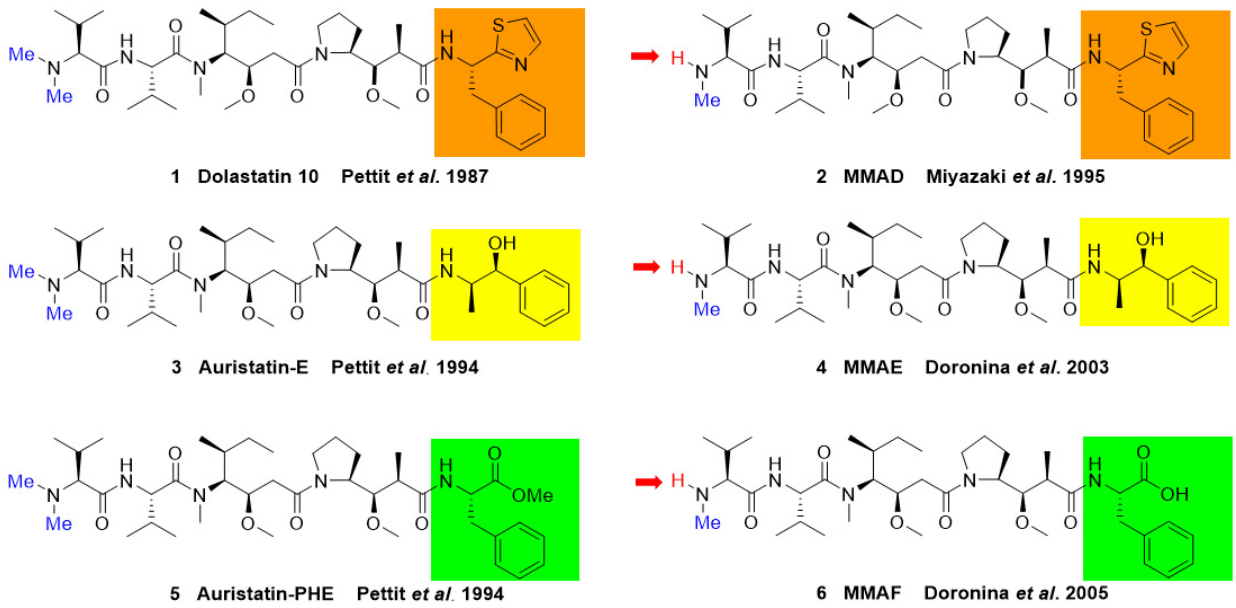

Figure 2. Structures of key auristatin analogs with three different C-termini. Top: Dolastatin 10 (**1**) and monomethyl auristatin-D (MMAD, **2**). Middle: auristatin-E (**3**) and monomethyl auristatin-E (MMAE, **4**). Bottom: auristatin-PHE (**5**) and monomethyl auristatin-F (MMAF, **6**). Color coding of C-termini: dolaphenine, (orange), (1*S*,2*R*)-(+)-norephedrine (yellow) and phenylalanine (green). Red arrow: removal of one *N*-Me group does not lead to significant potency loss.

Figure 2 shows key auristatin analogs containing the three different C-termini groups dolaphenine, (1*S*,2*R*)-(+)-norephedrine and phenylalanine. All three analogs were first described by Pettit. *et al*. as their *N*,*N*-dimethyl valine (dolavaline) N-termini constructs. [1,18,19] Miyazaki *et al*. discovered that removal of one methyl group from the N-terminal amine of the natural product Dolastatin 10 (**1**) gave mono-methyl auristatin-D (MMAD, **2**) and did not compromise *in vivo* antitumor activity. [14] This finding was later recognized by Senter *et al*., who made the

remarkable discovery that these auristatins having a secondary amine at their N-terminus could be attached to a linker and subsequently conjugated to monoclonal antibodies. This clever idea led to generation of highly potent and efficacious antibody-drug conjugates (ADC's).[20-22]

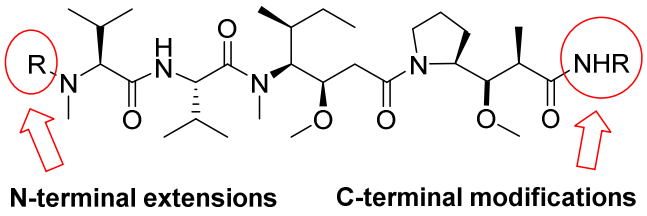

Figure 3. Hotspots for structural modifications of auristatin analogs.

Figure 3 displays the auristatin core structure and indicates the locations where the majority of chemical variations have been published. Notably, after the original publications of Pettit *et al.* and Miyazaki *et al*. most of the subsequent auristatin research has focused on analogs with C-terminal modifications and N-terminal extensions without modifications of the peptide structure (N-Me)Val-Val-Dil-Dap with only few exceptions.[14,23-28] Of particular note in this regard is the naturally occurring analog Symplostatin 1 that differs from Dolastatin 10 (**1**) by the presence of a terminal *N*,*N*-dimethylisoleucine instead of a terminal dolavaline residue.[3,29] The cytotoxicity of Symplostatin 1 is reported to be only slightly less when compared to **1**. To evaluate potential opportunities for structural modification, analysis of the detailed binding mode of the auristatins to tubulin is important. At the start of our studies, the only reported auristatin co-crystal structure using the [(Tc)2R] tubulin construct was obtained with the analog soblidotin (TZT-1027) (**7**, Figure 4)[15] by Cormier, Knossow *et al*..[6] The structure was disordered in some regions of the co-crystal complex but allowed for the basic assessment of the orientation and binding mode in the nucleotide exchange binding cleft of the tubulin construct used in this study. However, due to the

low resolution of the structure no detailed information of specific receptor interactions could be ascertained with good confidence. Nevertheless, when studying the co-crystal structure of **7** with tubulin, we noted a binding void around the N-terminus which suggested the potential for additional substitutions on the N-terminal carbon atom (Figure 4). We hypothesized that N-terminal amino acids with a α,α-dialkyl carbon substitutions could lead to potent new auristatin analogs. Additionally, we were interested in determining if changes on the N-terminus would lead to different *in vitro* ADME properties. Of particular interest was the potential modulation of *in vitro* intrinsic clearance profiles because our ultimate goal was to use these molecules as payloads for the next generation of antibody drug conjugates (ADC's).[22] The design rationale was that an ADC payload with high plasma clearance would be desirable, as this could reduce toxicity resulting from premature release of the payload from the antibody.

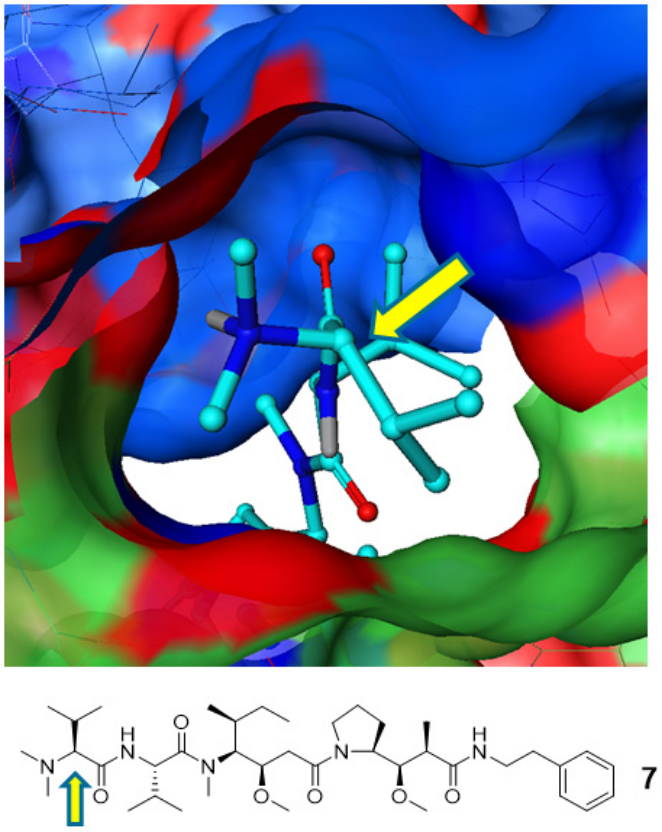

Figure 4. Co-crystal structure of soblidotin (TZT-1027) (**7**) with the (Tc)2R tubulin construct as described by Cormier, Knossow *et al*.[6] View of the N-terminus with the arrow indicating the N-terminal secondary carbon atom of interest. The structure of **7** is depicted with the correct stereochemical assignments as reported for **7** [15], but deviates from that reported in ref. 6, see text. A binding void is apparent in the receptor pocket that indicates the potential for further substitutions. Protein residues are displayed with their van der Waals radii and color coded based on atom type (dark blue: nitrogen, red: oxygen, light blue: beta subunit carbon, green: alpha subunit carbon). For the overall orientation of auristatin analogs at the α,β-tubulin interface see Figure 5 and ref. 6 .

Herein, we describe new N-terminal modifications with α,α-disubstituted amino acids that led to auristatin analogs with excellent potencies in tumor cell proliferation assays. We also present co-crystal structures of four analogs with tubulin having improved atomic resolution allowing for the first time the detailed examination of the auristatin binding mode. Furthermore, we investigate selected *in vitro* ADME characteristics of the new analogs and describe the pharmacokinetic profiling of the lead auristatin analog **20a** (PF-06380101).

CHEMISTRY

Pettit *et al*. first described the total synthesis of Dolastatin 10 (**1**) in 1989 and also described the preparation of the monomer building blocks dolaisoleuine (Dil), dolaproine (Dap) and dolaphenine (Doe).[5] Due to the interest in Dolastatin 10 (**1**) and related analogs, the preparation of the monomers has been improved over time. While there are multiple convergent methods of preparing the linear **1** molecule, Pettit *et al*. utilized the convergent method of separately preparing the left hand Dov-Val-Dil tripeptide (**8**) and right hand Dap-Doe dimer (**9**). [5,30,31]

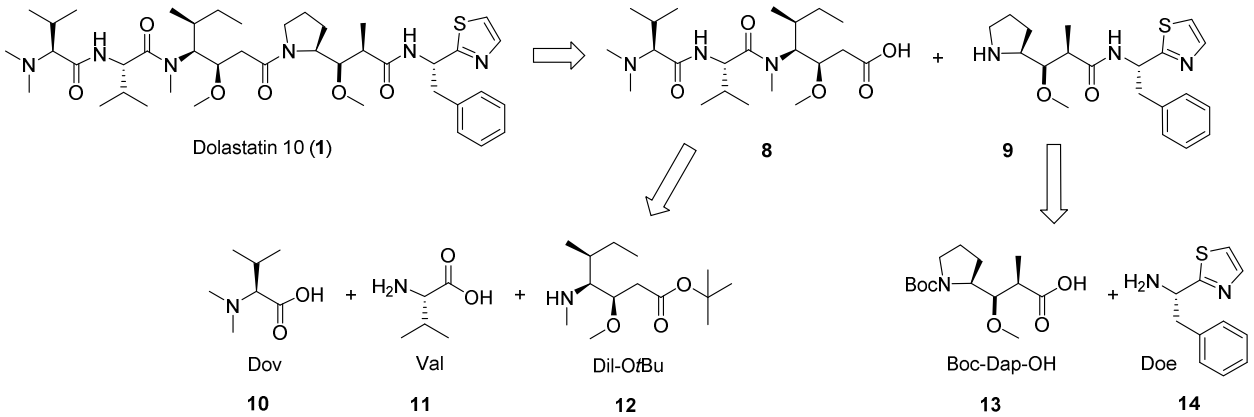

Scheme 1. Convergent synthesis of Dolalstatin 10 (**1**) based on tripeptide **8** and dimer **9**. [5]

We were interested in designing a flexible route that would allow for both N- and eventually C-terminal modifications in a modular fashion. For this purpose we sought to modify the synthetic route to enable introduction of the terminal amino acid at the last reaction step from **18**. Additionally, compound **18** could be generated by coupling of the dimers **15** and **16** (Scheme 2).

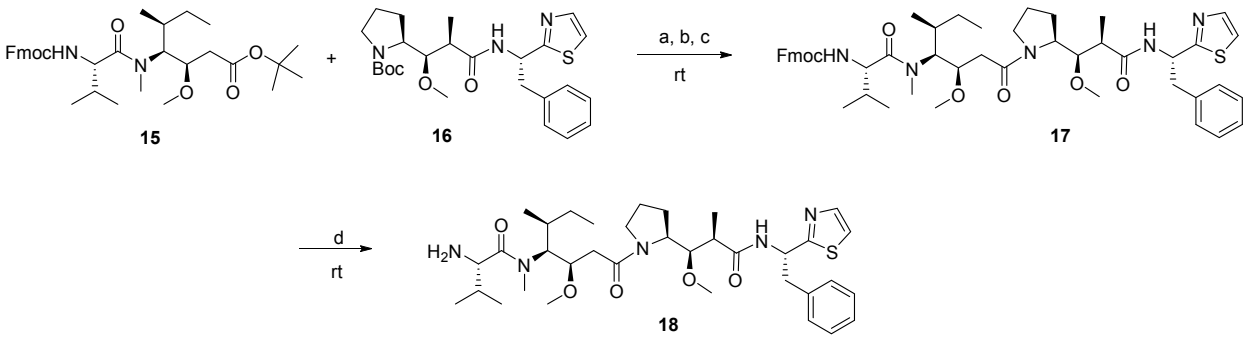

[a] Reagents and conditions: (a) TFA/DCM for **15** (b) HCl dioxane for **16** (c) HATU, *i*-Pr_2NEt, CH_2Cl_2, 78 % (d) Et_2NH, THF, rt, 87%.

Scheme 2. Synthesis of the tetramer Val-Dil-Dap-Doe (**18**) by using a modular approach from dimers **15** and **16**. Boc-protected **18** was previously prepared by an alternative method.[30,31]

The tetramer **18** was then utilized as a building block for the auristatin analogs as shown in Scheme 3. The amino acids **19 a-l** as their corresponding *N*-Boc or *N*-Fmoc protected analogs were coupled to the tetramer **18** using HATU with diisopropylethyl amine, then deprotected using either trifluoroacetic acid or diethylamine to give the auristatin analogs **20a-l**.

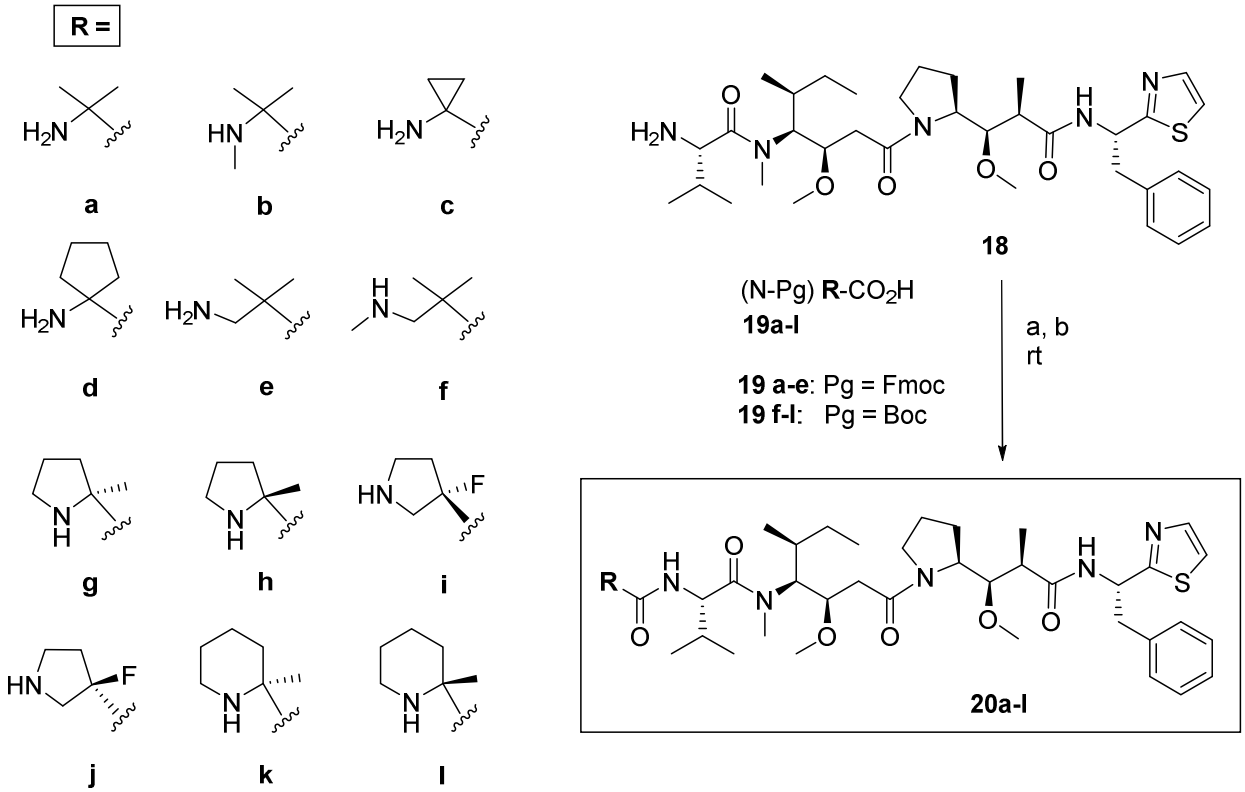

Reagents and conditions: (a) HATU, Et_3N, DMF; (b) Et_2NH, THF (**a-e**) or TFA, CH_2Cl_2 (**f-l**), (yields: 27-67% over two steps). N-Pg: protected amine.

Scheme 3. Synthesis of new auristatin analogs **20a-l**.

Additionally, three specific examples of the above auristatin analogs were prepared with phenylalanine as the C-terminus instead of the dolaphenine C-terminus (Scheme 4). For this purpose we applied similar chemistry procedures using the previously described tetramer Val-Dil-Dap-Phe-OMe (**21**).[32] This tetramer was coupled to protected Aib (**19a**), *N*-Me-Aib (**19b**) and (*S*)-2-methylpyrrolidine-2-carboxylic acid (**19g**) followed by saponification of the methyl ester and deprotection of the terminal amines.

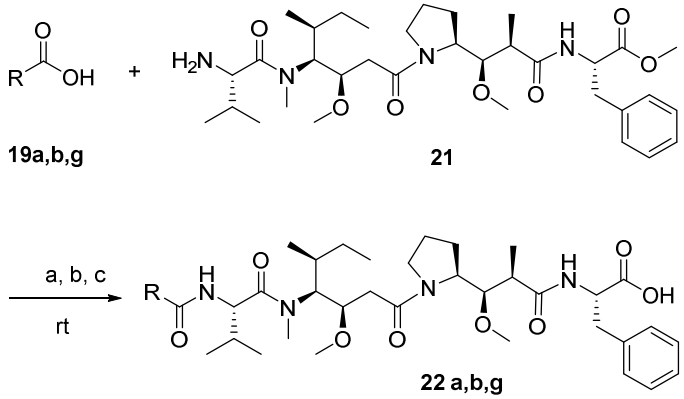

Reagents and conditions: (a) HATU, Et_3N, DMF (b) LiOH, MeOH and (c) TFA, CH_2Cl_2 (additional step for **22g**). Yields: 33-56% over two steps.

Scheme 4. Synthesis of new auristatin analogs **22a,b**,**g** containing a phenylalanine- instead of the dolaphenine C-terminus present in **20a-l**.

RESULTS AND DISCUSSION

Cell potencies of selected reference compounds and Aib-modified auristatins

Based on the crystal structure of **7** with tubulin, our hypothesis was that replacing the N-terminal amino acid of Dolastatin 10 (**1**) with an amino acid having two substituents at the α-position should be tolerated. However, it is well known that amino acids with two alkyl substituents at the α-position can lead to distortions of the peptidic structure due to induction of helical turns resulting from the Thorpe-Ingold effect, i.e. as exemplified with the amino acid Aib (2-aminoisobutyric acid).[33] The potential for success of this structural variation was non-obvious based on work by Miyazaki *et al*. who replaced the terminal dolavaline with *N*,*N*-dimethyl alanine and *N*,*N*-dimethyl glycine. Remarkably, the change from dolavaline to *N*,*N*-dimethyl glycine increased *in vivo* efficacy in xenograft studies, whereas *N*,*N*-dimethyl alanine at this

position completely abolished any efficacy.[14] This observation appeared to indicate the sensitive nature of the N-terminus with respect to structural modifications. Consequently, other positions on the peptide, i.e. the C-terminus, were deemed more favorable for potential structural modifications.[16,17] However, the interpretation of *in vivo* efficacy results in the absence of any data regarding cell-based potency, *in vitro* ADME and pharmacokinetics needs to be done with great caution. At the onset of our studies we investigated selected reference auristatins in tumor cell proliferation assays and two new analogs that contain 2-aminoisobutyric acid (Aib) at the N-terminus. GI_{50} values of cell viability were used as the primary potency readout taking into account all compounds in this manuscript showed good inhibition in the cell-free tubulin polymerization assay (data not shown). However, the tubulin polymerization assay generally requires significantly higher compound concentrations compared to cell based studies and is not suited for detailed SAR studies that examine subtle structural changes.[34] Of consideration is that cell potencies are a direct function of target affinity, cell-membrane permeability and potential active and passive transport processes, amongst other factors. It was determined that the passive cell permeability for all of the analogs prepared was generally low (RRCK cell line: P_{app} AB < 0.5 x 10^{-6} cm/sec),[35] and unless active uptake transport or other cell-uptake mechanisms (i.e. endocytosis) are involved, the cell GI_{50} values are likely driven by only a fraction of the extracellular compound concentration that is present inside of the cells. Hence, any change in observed cell potencies could reflect not just different tubulin binding affinities, but also altered cell permeability, cell uptake and transporter profiles. Of note is that none of the investigated cell lines described here had ABCB1 (MDR1) efflux transporters expressed. Having this limitation regarding cell based assay analysis in mind, BT474 cells (breast carcinoma), N87 cells (liver metastasis of gastric carcinoma) and MDA-MB-361-DYT2 cells (breast carcinoma) were

selected for the potency readout (Table 1). As expected, excellent potency was observed for the reference compounds MMAD (**2**), MMAE (**4**) and MMAF-OMe (**6**-OMe) (Figure 2) that all share the *N*-methyl valine N-terminus. To our surprise, the *N*-methyl glycine and *N*-methyl alanine analogs **23** and **24** retained good cell potencies despite the lack of the terminal isopropyl group. To the best of our knowledge, this is the first time that detailed cellular potencies are described for MMAD (**2**), the *N*-Me-glycine- (**23**) and *N*-Me- alanine (**24**) analogs. Gratifyingly, the new Aib analogs **20a** and **20b** having an α,α-geminal dimethyl group at the N-terminus showed a high degree of potency in all three investigated cell lines. Interestingly, the potency of these two compounds was not dependent on whether or not the terminal amino group was methylated. This stands in contrast to the corresponding N-terminal valine matched pair **2** (MMAD) and **25**, where the absence of the N-methyl group in **25** led to a significant reduction in potency.

ID	BT474 [nM]	MDA-MB-361-DYT2 [nM]	N87 [nM]
4 (MMAE)	**0.22** (± 0.15, 9)	**0.49** (± 0.15, 15)	**0.54** (± 0.35, 22)
6-OMe (MMAF-OMe)	**0.24** (± 0.18, 24)	**0.21** (± 0.15, 14)	**0.44** (± 0.54, 20)
2 (MMAD)	**0.12** (± 0.094, 12)	**0.090** (± 0.013, 6)	**0.30** (± 0.22, 13)
23	**0.49** (± 0.15, 3)	**0.69** (± 0.26, 3)	**1.2** (± 0.39, 3)
24	**0.23** (± 0.014,3)	**0.25** (± 0.081, 4)	**0.42** (± 0.15, 4)
25	**5.3** (± 0.91, 3)	**9.0** (± 2.4, 2)	**10** (± 2.2, 2)
20a (PF-06380101)	**0.26** (± 0.37, 16)	**0.19** (± 0.073, 19)	**0.27** (± 0.16, 18)
20b	**0.045** (± 0.012, 3)	**0.076** (± 0.047, 4)	**0.12** (± 0.10, 4)

Table 1. Cell potency in tumor cell viability assays expressed in GI_{50} values with two significant figures as arithmetic means in nanomolar concentrations. Standard deviations and the count of individual assay runs (n). Each individual assay run is a duplicate readout. N-terminal amino acids: **23**: *N*-Me-L-glycine, **24**: *N*-Me-L-alanine, **25**: L-valine, **20a**: aib, **20b**: *N*-Me-aib. Aib: 2-aminoisobutyric acid.

Crystal structure analysis of 20a (PF-06380101)

Encouraged by the excellent cell potency of **20a** (PF-06380101) we sought to further analyze the binding mode by crystallography using the (Tc)2R tubulin construct.[6] Numerous tubulin crystal structures have been published, most notably by elegant work from Gigant, Knossow *et al*. [6,36,37] These structures give insight into the mechanism of polymerization of tubulin as well as the method of inhibition of polymerization *via* co-structure with various inhibitor classes. For most of these co-structures, the resolution is between 3.5Å and 4Å. This low resolution limits the clarity of which the interaction with tubulin can be visualized with these inhibitors. In the case of the auristatin compound soblidotin (TZT-1027) (**7**), examination of the structure and data deposited in the Protein Data Bank (Entry 3E22) show that the last two C-terminal residues are disordered at 3.8Å and cannot be placed with confidence.[6] Recent advances in tubulin crystallography have provided crystals that diffract to significantly higher resolution prior to soaking compounds.[38] Using this new information, we undertook the structure determination of auristatin compounds bound to tubulin with the goal of providing a higher resolution co-structure to aid our structure based design of tubulin inhibitors. This work is exemplified by the co-structure of tubulin with **20a**, which was solved at an improved 3.1Å resolution.

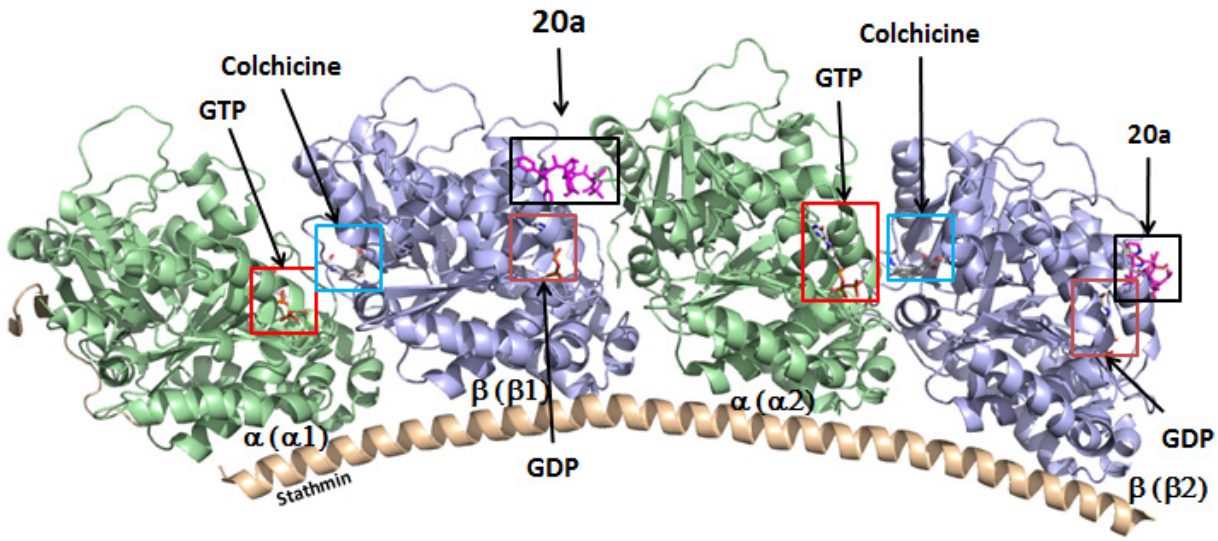

Figure 5. Co-crystal structure of **20a** with the (Tc)2R tubulin construct. Overview of the binding mode with relative orientation of construct components. **20a** binds at the α,β-tubulin interface. A second molecule of **20a** is also associated with the exterior β-subunit. PDB code 4X1I.

As previously described by Cormier *et al*., the binding site of auristatins is in close proximity to the β-tubulin nucleotide exchange region and the auristatin binding event leads to direct interference with the GTP/GDP hydrolysis process resulting in compromised tubulin polymerization and mitotic arrest (Figure 5).[6] In the co-structure of **20a**, all residues of the compound can be fit-to-density and as a result the examination of the interaction of this compound with tubulin was possible with greater clarity than in the 3.8Å structure solved by Cormier *et al.*.[6]

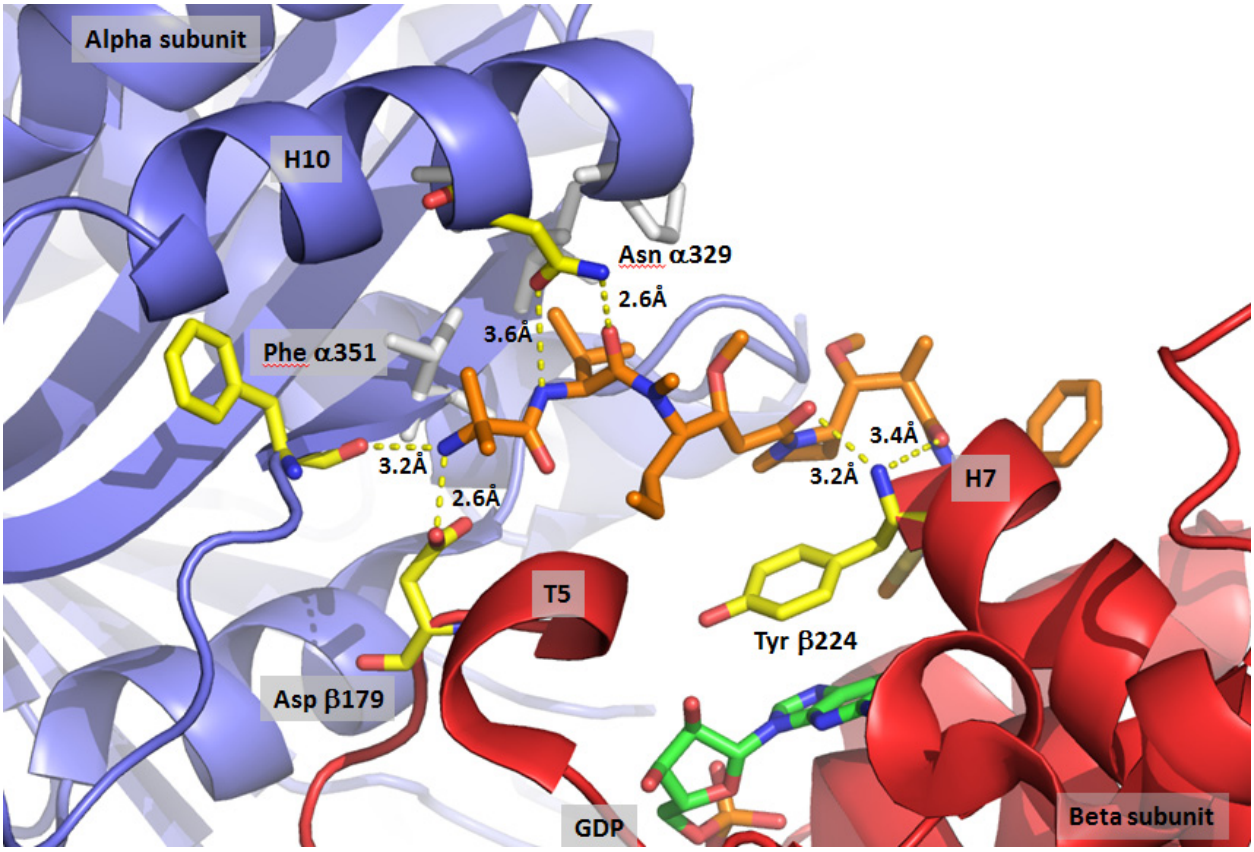

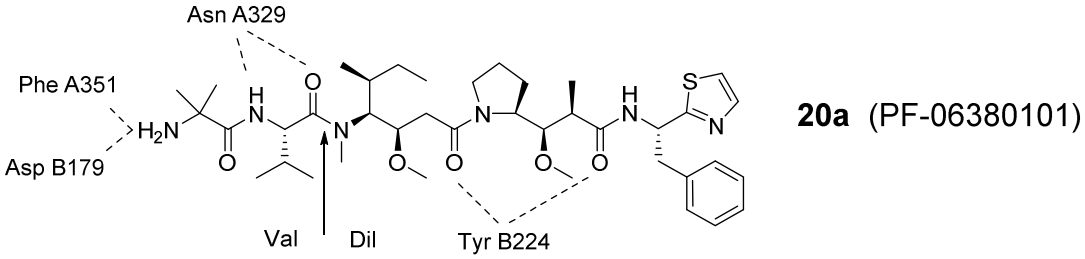

20a (PF-06380101)

Figure 6. Binding mode of **20a** observed in the 3.1Å co-structure with tubulin with selected key receptor interactions at the N-terminus. Red: β-subunit, blue: α-subunit, GDP in green. For simplicity the structure of **20a** is drawn with *trans*-configuration of the Val-Dil amide bond

(indicated with arrow), but in the co-crystal structure the Val-Dil amide bond of **20a** bound at the tubulin β1/α2 interface has *cis*-coniguration, see text. PDB code 4X1I.

In this higher resolution tubulin-**20a** co-crystal structure (Figures 5,6), the protein chain tracings are identical to that which has been described previously with the T5 loop flipped out, exposing Asp β197 to solvent.[6] This movement of the T5 loop is required when compounds bind in the vinca domain peptide region and is regularly observed. Upon insertion of an entity into the vinca domain region, additional curvature is induced into the protein assembly. For example, atoms in β-2 subunit move by almost 3Å and the C-terminal residues of the stathmin domain move by over 5Å. It is presumably this inhibitor-induced curvature that is the basis for the diffraction sensitivity of the soaked protein crystals. The Aib N-terminus is easily accommodated in this pocket and slightly larger groups can be tolerated. The N-2 valine interacts with the β-1 subunit by inserting into a large pocket formed by the side chains of Val177, Tyr210 and Leu227 (not shown). Notable polar interactions include a hydrogen bond network between the terminal protonated amino group with Asp β197 located on the T5 loop and the amide carbonyl of Phe α351, a bifocal interaction of the N-2 valine with Asn α329 and a critical hydrogen bond interaction between the backbone amide of Tyr β224 with the terminal carbonyl groups of Dap and Doe in **20a**. This latter hydrogen bond network arranges the aromatic ring Tyr β224 in a π-stacking interaction with the nucleobase of GDP, preventing it's dissociation from β-tubulin. The trapping of GDP is believed to be a key mechanism by which auristatins exert their tubulin-interfering effect. As stated above, the remaining residues including the C-terminus interact primarily with the β-tubulin subunit and their mode of binding arranges the peptide such that the carbonyl associated with the final residue is located at the tip of helix H7 aligned with the helix dipole (Figure 7).

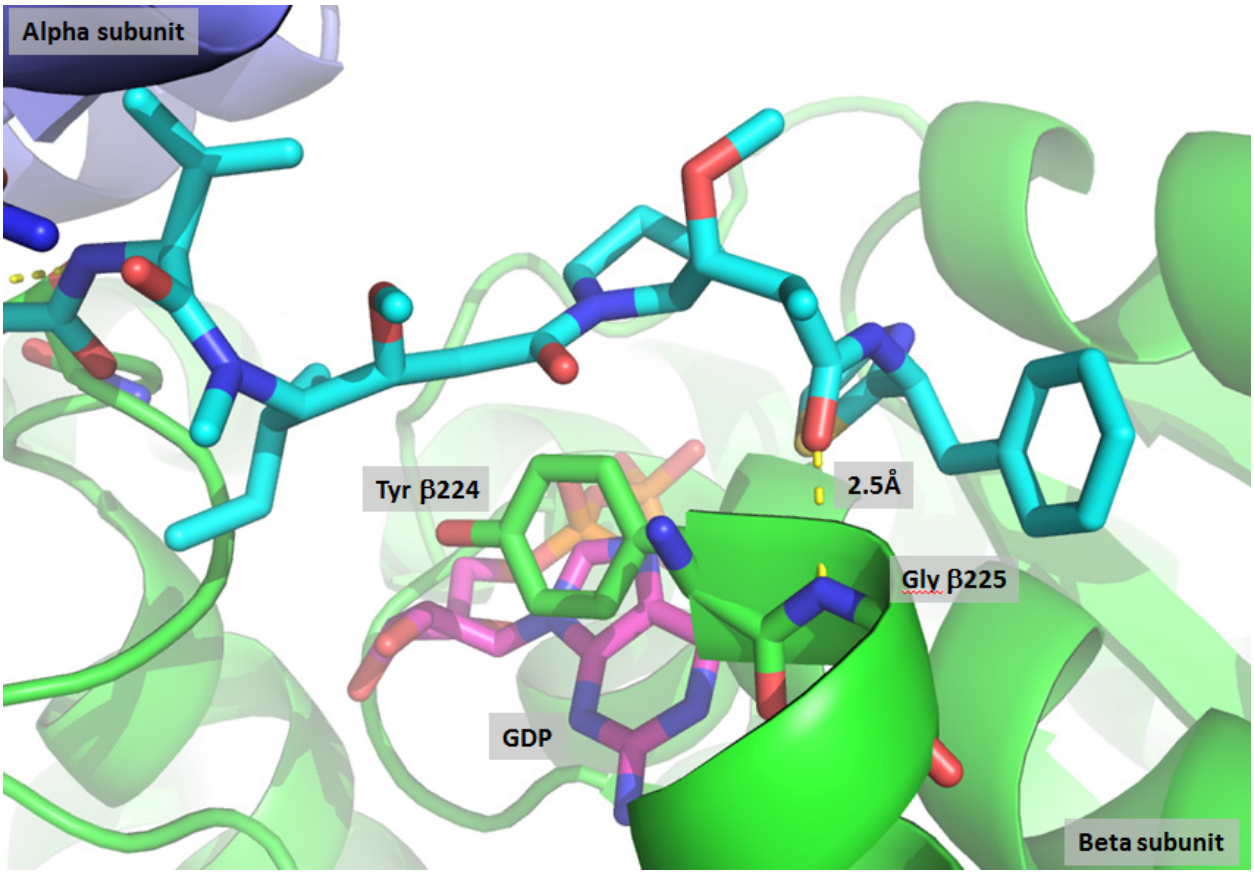

Figure 7. Binding mode of **20a** observed in the 3.1Å co-structure with tubulin, view on the C-terminus. PDB code 4X1I.

In addition to the molecule of **20a** found at the interface of the β1 and α2 subunits, a second molecule of **20a** is bound unproductively to the distal β2 subunit (Figure 5). There is no alpha subunit associated with the β2 subunit but the compound interacts with the beta subunit in a similar way as seen at the internal alpha/beta interface.

Configurational analysis

We do observe a major configurational difference between the two bound molecules **20a**, as the **20a** molecule found at the β1/α2 tubulin interface has a *cis*-configuration near the N-terminus between the amino acids Val-Dil while the compound associated with β2 tubulin has *trans*-configuration at the Val-Dil amide bond. Superimposing the beta subunits and examining the fit-to-density for the compounds shows that this difference is real. By adopting the *cis*-configuration **20a** is able to provide complementary interactions to Asn α329 as seen in Figure 6. These interactions are not possible if the Val-Dil amide bond has *trans*-configuration. The lack of a corresponding α subunit for the exterior copy of **20a** explains why the *cis*-configuration in the second **20a** molecule is not observed.

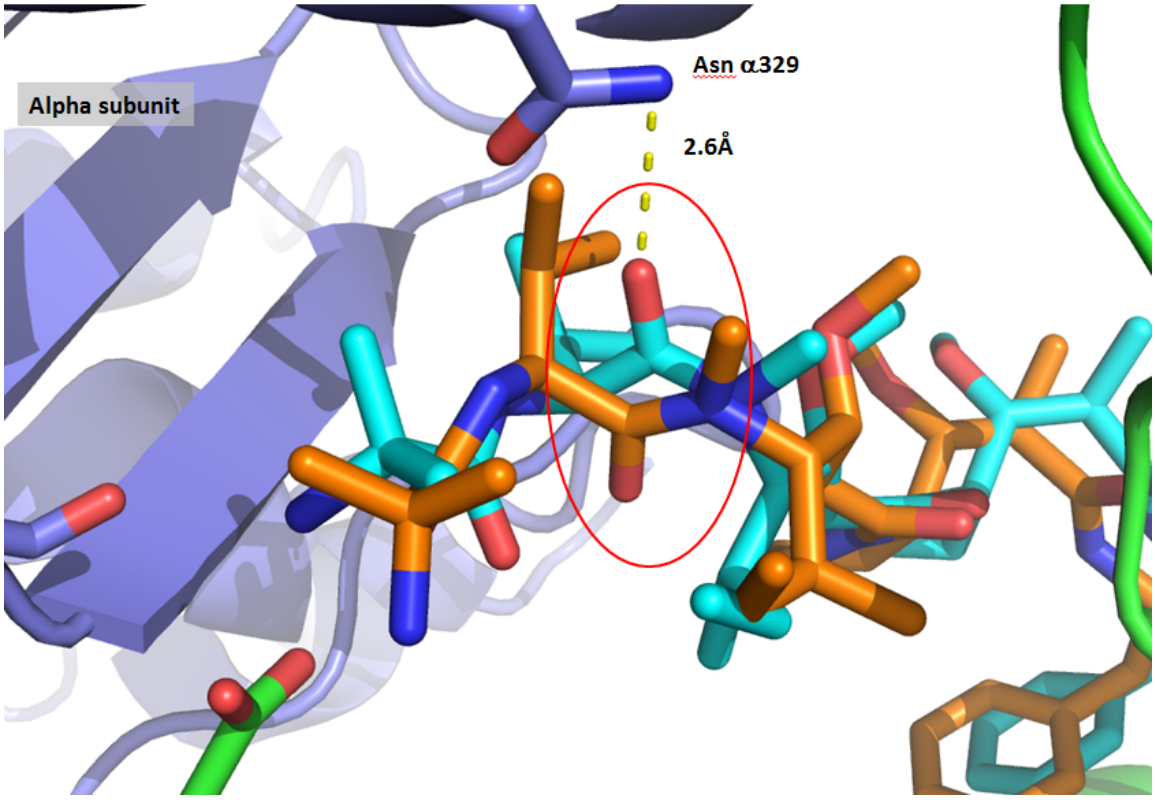

Figure 8. The configurational differences between the valine (Val) and dolaisoleuine (Dil) residues of compound **20a**, as observed at the β1/α2 tubulin interface (cyan) and observed bound to β2 tubulin (orange), is highlighted by the red circle. Only in the *cis*-configuration the carbonyl of the valine residue is able to make a productive interaction with Asn α329 from the α2 subunit. PDB code 4X1I.

An important observation is that the Val-Dil amide bond of **20a** in solution has *trans*-configuration, with no observable *cis*-isomer detected by NMR at room temperature (DMSO), whereas the amide bond in between Dap and Dil is a mixture of both *trans*- and *cis*-rotamers. However, in the tubulin co-crystal structure the Val-Dil bond amide bond of the functionally relevant bound form of **20a** at the β1/α2 tubulin interface is seen to be in *cis*-configuration. At first glance this might be surprising since none of this form seems to be present in solution as detected by NMR, suggesting the energy difference between *trans*- and *cis* forms is greater than 2.7 kcal/mol. For tertiary amides the barrier to rotation around the amide bond is often 17-20 kcal/mol.[39] At this energy it is still possible to access both *trans*-and *cis*-forms kinetically since the exchange between *trans*- and *cis*-forms by rotation around the amide bond is in the msec to sec range. Thus, tubulin can select the most favorable form giving the lowest overall ΔG of binding. Apparently, the energy expenditure for the rotation of the Val-Dil amide bond in **20a** from *trans* (solution state) to *cis* (tubulin bound) is more than compensated for by the resulting high binding energy of **20a** having picomolar dissociation constants (tubulin binding assay by fluorescence polarization, data not shown). Interestingly, the other unproductively bound molecule of **20a** appears to not make favorable interactions with tubulin and it remains associated in its *trans* form as previously shown. This is in agreement with two studies by Alattia *et al*. and Benedetti *et al*. who investigated the NMR solution structure of **1**.[40,41] In addition, the

crystallographic analysis of the tubulin-unbound isodolastatin 10, an epimer of **1**, also only showed the *trans*-configuration between Val and Dil.[42] It is interesting to speculate what the binding energy would be in analogs having pre-organized *cis*-amide bonds at the Val-Dil juncture.

Activities of additional N-modified analogs

Based on the structural information obtained with **20a** additional new analogs with N-terminal modifications were explored (Table 2). In particular, there was an interest to investigate how various cyclic motifs would be tolerated at the N-terminus and whether the configuration of the stereocenter present in the chiral amino acids would influence potency. Also, β-amino acids represented by **20e**,**f** and fluorine containing analogs **20i**,**j** were prepared to determine the impact of these modifications on activity. Table 2 indicates that all prepared compounds showed good cell-based potencies comparable with those of MMAE (**4**) and MMAF-OMe (**6**-OMe) with only subtle differences. However, as pointed out previously, the high activity of **20a** (PF-06380101) is notable in that it possesses a primary amine, a trend that is not observed for the natural valine N-terminus present in MMAD **(2)**, where the N-Me group is necessary for potency (see matched molecular pair **2** and **25**, table 1).

ID	BT474 [nM]	MDA-MB-361-DYT2 [nM]	N87 [nM]
4 MMAE	**0.22** (± 0.15, 9)	**0.49** (± 0.15, 15)	**0.54** (± 0.35, 22)
6-OMe (MMAF-OMe)	**0.24** (± 0.18, 24)	**0.21** (± 0.15, 14)	**0.44** (± 0.54, 20)
2 (MMAD)	**0.12** (± 0.094, 14)	**0.090** (± 0.013, 8)	**0.30** (± 0.22, 13)
20a (PF-06380101)	**0.26** (± 0.37, 16)	**0.19** (± 0.073, 19)	**0.27** (± 0.16, 18)
20b	**0.045** (± 0.012, 3)	**0.076** (± 0.047, 4)	**0.12** (± 0.10, 4)
20c	**2.9** (± 1.1, 5)	**5.6** (± 1.6, 2)	**6.4** (± 3.8, 4)
20d	**0.28** (± 0.11, 10)	**0.35** (± 0.20, 8)	**0.33** (± 0.14, 10)
20e	**0.25** (± 0.10, 3)	**0.81** (± 0.49, 3)	**1.4** (± 1.5, 3)
20f	**0.25** (± 0.058, 3)	**0.41** (± 0.19, 3)	**1.1** (± 0.53, 3)
20g	**0.14** (± 0.019, 3)	**0.20** (± 0.19, 4)	**0.15** (± 0.036, 3)
20h	**0.11** (± 0.040, 3)	**0.21** (± 0.11, 3)	**0.36** (± 0.15, 3)
20i	**0.16** (0.019, 3)	**0.25** (± 0.069, 3)	**0.59** (± 0.33, 3)
20j	**0.29** (± 0.057, 3)	**0.60** (± 0.24, 3)	**1.1** (± 1.7, 3)
20k	**0.16** (± 0.023, 3)	**0.20** (± 0.11, 3)	**0.25** (± 0.16, 3)
20l	**0.35** (± 0.091, 3)	**0.40** (± 0.011, 3)	**0.52** (± 0.22, 3)

Table 2. Cell potency in tumor cell viability assays of additional auristatin analogs expressed in GI_{50} values with two significant figures as arithmetic means in nanomolar concentrations. Standard deviations and the count of individual assay runs (n). Each individual assay run is a duplicate readout.

The β-amino acid versions **20e** and **20f** are only slightly less potent than the corresponding α-amino acid counterparts **20a** and **20b** in the DYT2 and N87 cells, once again showing little influence of the N-methylation status on potency. The cyclopropyl analog **20c** is less active than the cyclopentyl derivative **20d**. Of note are the high activities of the pyrrolidine and piperidine analogs (**20g**,**h** and **20k**,**l**) with seemingly no influence of the configuration of the stereocenter, once more highlighting that structural modifications on the N-terminus are possible without compromising potency.

Crystal structure analysis of 22a, 22b and 22g

The good activity of the N-terminal pyrrolidine was predicted based on the analysis of the crystal structure of **20a**, which suggested that five and six-membered saturated rings could be tolerated in the binding pocket that accommodates the auristatin N-terminus. Critical receptor interactions of **20a** were identified to be the hydrogen bond network of the primary amino group in **20a** with the Asp β179 located on the T-5 loop, the carbonyl backbone of Phe α351 as well as the bifocal interaction with Asn α329. Figure 9 shows the superimposed co-crystal structures of **22a** and **22g** allowing the direct comparison of the binding mode of the respective N-termini. For both compounds the C-terminus was chosen to be phenylalanine instead of dolaphenine to facilitate the crystallization. This change in the C-terminus did not perturb the overall binding

conformation of the auristatin peptide. The inspection of Figure 9 reveals that the overall binding mode of **22a** and **22g** is very comparable with good alignment of both bound conformations. Of particular interest is that in both compounds the N-termini engage in the Asp β179, Phe α351 and Asn α329 hydrogen bond network. Both analogs retain high tubulin binding affinity at a level comparable to that of the dolaphenine analogs **20a** and **20g** (data not shown). Detailed cell-free tubulin binding affinity studies using a newly developed fluorescence polarization competition assay will be described in a subsequent publication.

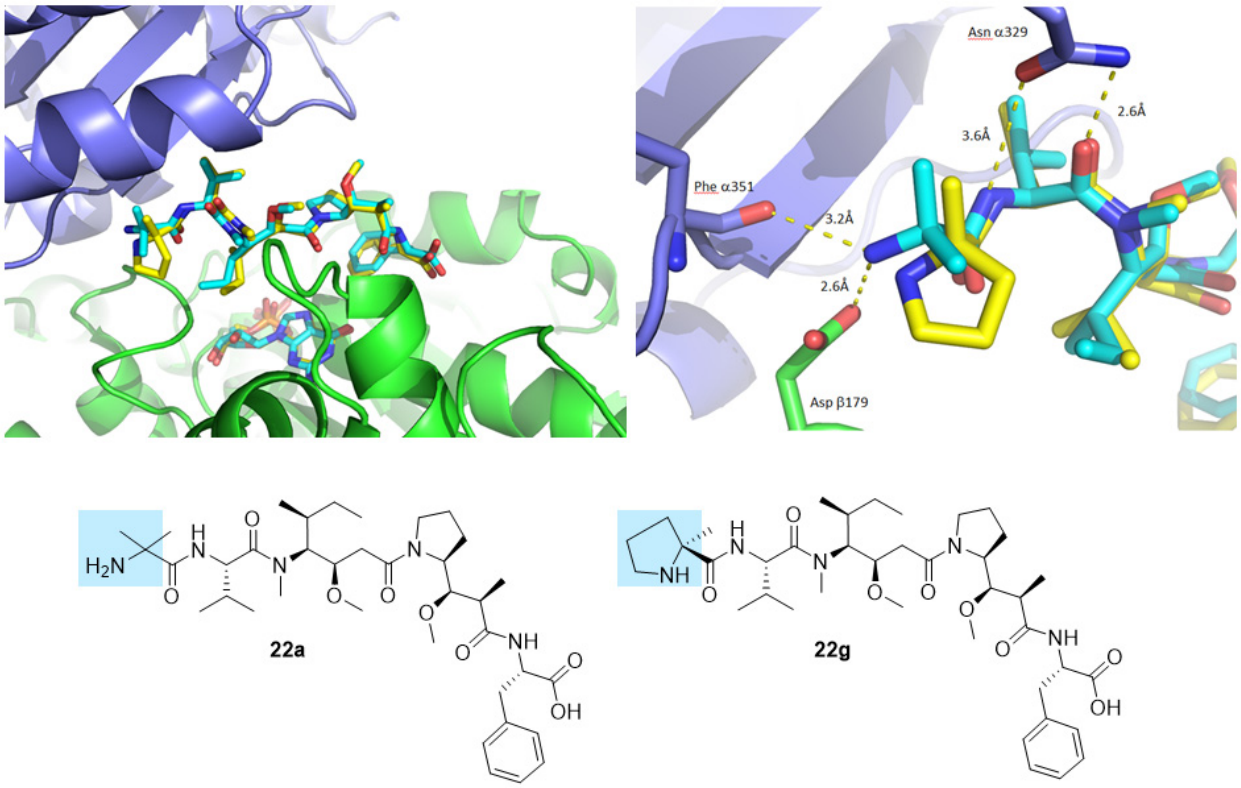

Figure 9. Overlayed co-crystal structures of **22a** and **22g**. Left: structure complexes in the binding domain superimposed and showing entire peptide structures of **22a** and **22g**. Right: close-up view of N-terminus. Visible is the critical hydrogen bond network of both N-termini with Asp β179, Phe α351 and Asn α329, interactions that are preserved in both molecules and

believed to be important for binding affinity. The Val-Dil amide bonds are in *cis*-configuration. RDB codes: 4X1K (**22a**), 4X20 (**22g**).

Figure 10 shows the N-terminal view of the superimposed co-crystal structures of **22b** and **22g** . The analog **22b** differs from **22a** by the presence of a secondary *N*-Me amino group which does not compromise the hydrogen network of the terminal amino group with Asp β179, Phe α351 and Asn α329. Of particular note is the difference in the relative orientation of the methyl group in **22g** as compared to the position of both geminal dimethyl groups in **22a** and **22b**. The *N*-methyl group in **22b** adjusts the positioning of the N-terminus of the compound relative to **20a**. The N-terminal nitrogen moves ~2Å and the *N*-methyl group is vectored into a channel between the α and β subunits. This vector is one that can easily accommodate large linear groups.

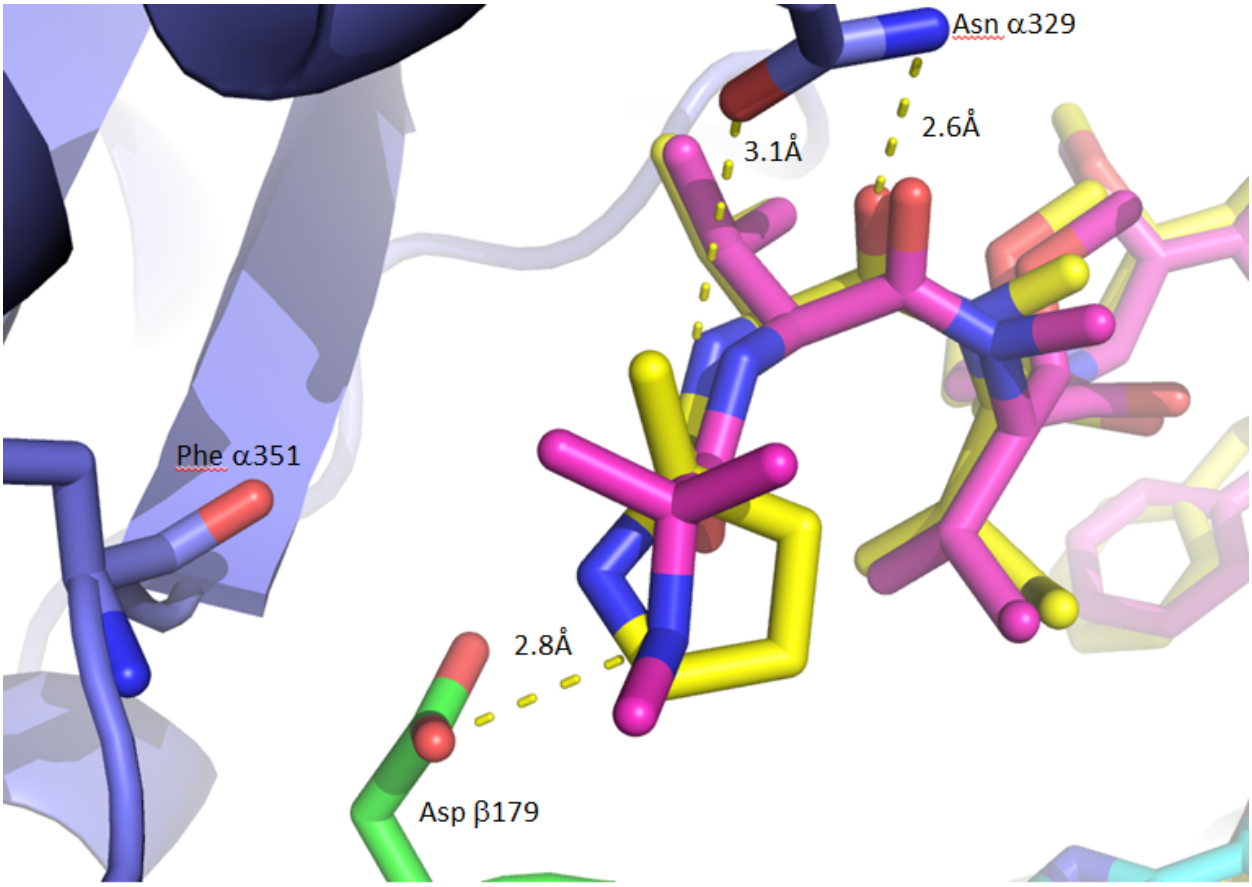

Figure 10. Overlayed co-crystall structures of **22b** and **22g**, view of the N-terminus. Notable is the relative orientation of the pyrrolidine Me-group and the two geminal methyl groups in **22b**. In both analogs the Val-Dil amide bonds have *cis*-configuration and engage with Asn α329 via bifocal interaction. RDB codes: 4X1Y (**22b**), 4X20 (**22g**).

It should be noted that in the deposited structure of soblidotin (TZT-1027) (**7**), the Val-Dil amide bond is in the *trans*-configuration. In contrast, the Val-Dil amide bonds in the functionally relevant tubulin-bound structures of all the four auristatin analogs (**20a**, **22a**, **22b** and **22g**) presented here are in the *cis*-configuration. In addition to this discrepancy, in the published crystal structure of **7** three chiral centers (positions 9, 18 and 19a) have different stereochemical assignments than those originally reported for **7**.[14,15] In contrast, all compounds described here

have stereochemical assignments that are consistent with those published for Dolastatin 10 and other auristatin analogs. The unexpected finding of the *cis*-configured Val-Dil amide bond in all crystallized analogs described here, that have a functionally relevant binding mode at the β1/α2 tubulin interface, is remarkable and reveals a preferred auristatin binding mode that was not previously recognized for this compound class. The high potency and conserved binding modes of the described N-terminal analogs highlight how structural modifications at the N-terminus can be tolerated without loss of binding affinity. This is also apparent when inspecting the cell-based potencies of the pyrrolidine epimers **20g** and **20h** as well as the piperidine epimers **20k** and **20l** which indicate that inversion of the pyrrolidine or piperidine stereocenter does not compromise target affinity or cell based activities.

In summary, all new compounds show an appreciable amount of activity when compared to the benchmark auristatins with very little variation in cell-based potencies. This result is surprising as previous studies suggested that the N-terminal modifications would be less tolerated. All investigated compounds have generally low passive cell-membrane permeability with only minor differences (data not shown). Potential explanations for the high cell-potencies, despite the poor passive cell-membrane permeability, include the possibility for active uptake mediated by transporters or endocytosis pathways that have been previously described for peptides.[43] It also remains a possibility that the high cell activity is caused by only a fraction of the drug that penetrates the cell-membrane by passive permeation.

Human liver microsome intrinsic clearance

Upon profiling of new analogs using an *in vitro* ADME panel it was observed that all new compounds with α,α-di-substitution showed significantly elevated human liver microsome (HLM) apparent intrinsic clearance values (Figure 11).[44]

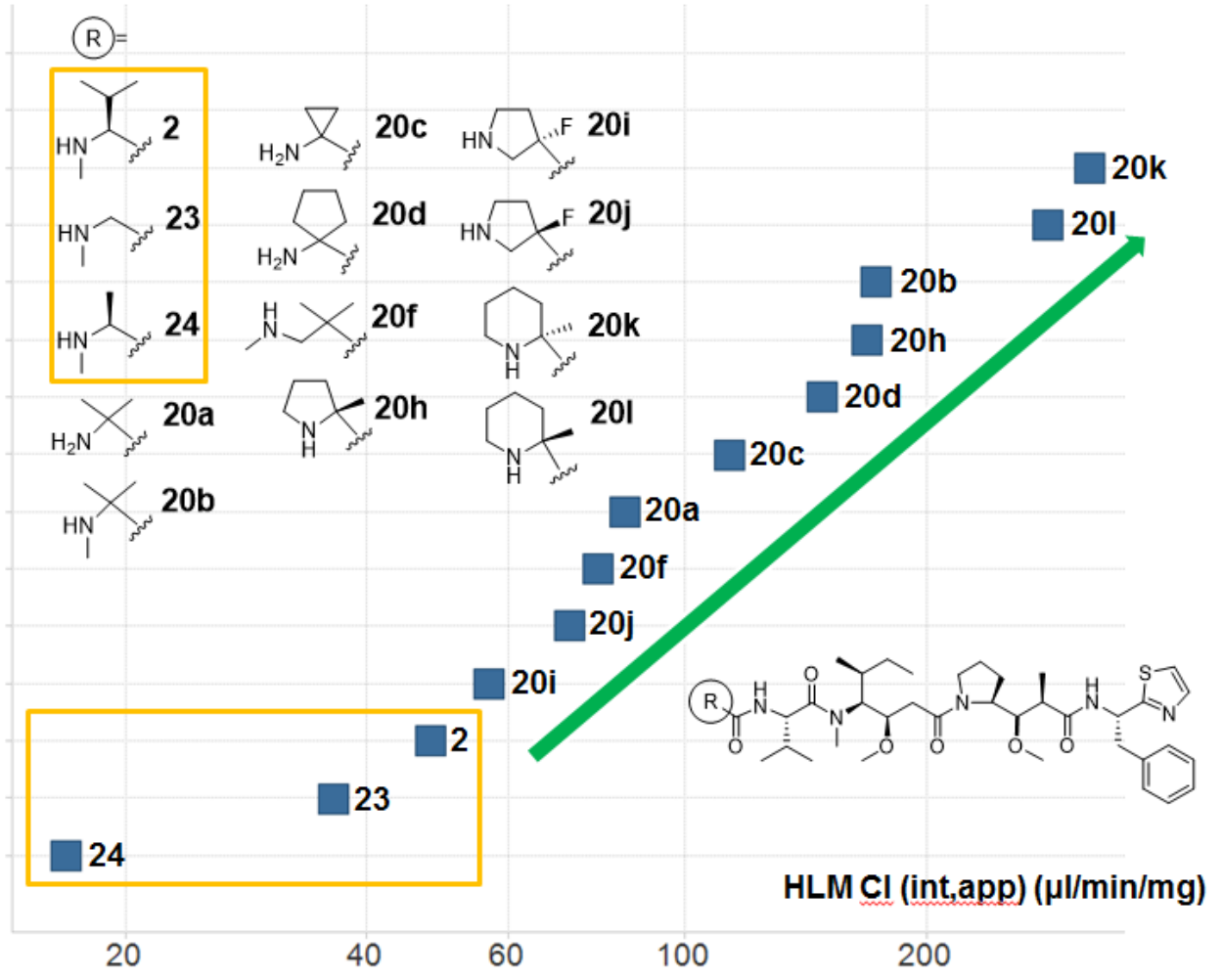

Figure 11. X-axis: log scale, human liver microsome (HLM) apparent intrinsic clearance values of selected analogs [µl/min/mg], dose: 1µM. Y-axis: Compound row number, without dimension. Compounds in the yellow box are compounds with reference N-termini. Significant increase in

HLM clearance values for new analogs was recorded and is graphically represented by the green arrow.

Of particular interest are the matched molecular pairs **2/20b, 23/20b** and **24/20b**. These pairs only differ at the N-terminal α-carbon atom, with **2**, **23** and **24** having a primary and secondary α-carbon atom and **20b** having a tertiary α-carbon atom. The significant increase in the HLM values in these matched pairs from moderate levels (HLM: 17-50) to very high levels (HLM: 173) is remarkable given the only small structural variation present in **20b**. It was reported that MMAE (**4**), the auristatin payload present in the antibody drug conjugate (ADC) brentuximab vedotin, is mainly cleared by liver oxidative metabolism mediated by CYP3A4.[45] In a clinical study it was found that co-dosing of brentuximab vedotin with the CYP3A4 inducer rifampin led to significantly reduced plasma concentrations of unconjugated MMAE (**4**) payload.[45] This data establish a direct correlation between the intrinsic clearance capacities of the CYP P450 enzymes with clinical plasma exposure levels of MMAE (**4**). Considering the high cytotoxicity of the auristatins, one desirable goal of developing antibody drug conjugates is to minimize systemic payload exposure after ADC dosing. In this regard, auristatins with rapid clearance from systemic circulation could provide a safety advantage. Even though the systemic plasma payload exposure after ADC dosing is generally very low compared to the corresponding ADC, the absolute exposure values of the unconjugated payload can nevertheless significantly exceed its GI_{50} values in cell viability assays, even when corrected for plasma protein binding. Hence, the contribution of free payload to general toxicity can't be underestimated and is a true concern. The relationship between CYP P450 clearance capacity, systemic plasma exposure and toxicity has been clearly established for chemotherapeutics such as docetaxel, which is also cleared by oxidative hepatic metabolism like MMAE (**4**) and **20a**.[46] In this regard, it is important to

understand if active metabolites exist. These studies are currently ongoing with **20a** and related analogs and will be reported in due course. Table 4 shows a direct comparison of **20a**, MMAD (**2**) and MMAE (**4**) with respect to apparent intrinsic clearance values obtained with human liver microsomes and human liver hepatocytes. The comparison shows that **20a** has the highest intrinsic clearance values compared to MMAE (**4**) and MMAD (**2**) in both human microsomes and human liver hepatocytes.

	HLM Cl(int, app) [µl/min/mg]	HHEP Cl(int, app) [µl/min/million]
20a	84	21
2 MMAD	48	11
4 MMAE	24	3

Table 3. Apparent intrinsic clearance values of **20a** (PF-06380101), MMAD (**2**) and MMAE (**4**) with human liver microsome (HLM) and human liver hepatocytes (HHEP). Dose: 1 µM.

For the selection as an ADC payload many parameters are important in addition to intrinsic clearance profiles. The full selection criteria, in particular in context of compound **20a**, will be reported in a future publication.

Pharmacokinetic analysis of 20a (PF-06380101)

After an IV dose of **20a** at 20 μg/kg to Wistar Han rats, **20a** exhibited a mean systemic clearance (Cl) of 70 mL/min/kg and a volume of distribution (V_{ss}) of 14.70 L/kg, resulting in a terminal elimination half-life (t ½) of approximately 6 hours (Table 4). Following repeat IV dosing of **20a** to Wistar Han rats, mean systemic exposure increased with increasing dose. Mean C_{max} and AUC ratios on Day 29 relative to Day 1 were generally similar with ratios (Day 29 / Day 1) less than 2.0, suggesting there was no accumulation of **20a** observed over the dosing interval. **20a** was moderately to highly bound to plasma proteins (fraction unbound fu at 0.1 uM dose is 0.24 for monkey, 0.10 for rat and 0.07 for human plasma).

C_{max} (ng/ml)	19.4 ±2.16
T_{max}	0.14 ± 0.050
AUC_t (ng*h/ml)	4.51 ± 1.14
Cl (ml/min/kg)	70.0 ± 12.8
V_{SS} (L/kg)	14.70 ± 3.05
$t_{1/2}$ (hours)	5.85 ± 1.17

Table 4. Pharmacokinetic parameters for **20a** after a single iv dose of 20 μg/kg in male Wistar Han Rats (n = 3) determined by LC-MS/MS. AUC_t = area under the concentration time curve from time zero to the last measurable concentration calculated; Cl = systemic serum clearance;

C_{max} = observed peak concentration; $t_{½}$ = apparent terminal elimination half-life; T_{max} = observed time to reach C_{max}; Vss = apparent volume of distribution.

After a single 36 μg/kg IV dose (bolus) of **20a** to Wistar Han rats (n = 3) and Sprague-Dawley rats (n = 3), approximately 8% of **20a** dose was recovered in urine, and approximately 4% in bile, respectively. *In vitro* studies with non-radiolabeled compound suggest that **20a** preferentially distributes into human plasma relative to whole blood and that **20a** is a P-glycoprotein (P-gp) substrate. A preliminary assessment of the metabolism of **20a** using non-radiolabeled compound was conducted using rat, monkey and human liver S9 fractions and human recombinant cytochrome P450 (rCYP) enzymes. All metabolites were oxidative in nature and β-nicotinamide adenine dinucleotide phosphate (NADPH)-dependent, with no amide hydrolysis products or glucuronide conjugates observed. There was no evidence of human specific metabolites. Initial reaction phenotyping experiments suggest that CYP3A4 is the predominant enzyme involved in the metabolism of **20a** with hydroxylation occurring on the N-terminus. Based on the *in vitro* drug-drug interaction (DDI) studies (direct inhibition, metabolism-dependent inhibition, and induction), **20a** is anticipated to be of low risk to perpetrate pharmacokinetic drug interactions with compounds for which CYP1A2, CYP2B6, CYP2C8, CYP2C9, CYP2C19, CYP2D6, and/or CYP3A4/5-mediated metabolism constitutes the primary mechanism of clearance. However, since **20a** is primarily metabolized by CYP3A4, there is potential for DDIs if co-administered with moderate and/or potent clinical inhibitors and/or inducers of CYP3A4.

In summary, we have described the design and synthesis of several auristatin analogs with N-terminal modifications that include amino acids with α,α-disubstituted carbon atoms. This modification of the peptide structure is unprecedented and led to analogs with excellent

potencies in tumor cell proliferation assays. All new analogs show good potency with only subtle differences in activities. We have disclosed, for the first time, auristatin crystal structures with improved resolution further enabling the detailed examination of their binding modes. The analysis revealed that the N-terminal geminal dimethyl groups present in **20a** (PF-06380101) and **20b** are well accommodated in the receptor pocket without compromising the overall binding affinity of the molecules. In particular, key interactions were identified that allowed the subsequent design of active analogs. Critical interactions that were conserved for all analogs include the H-bond network with Asp β179 and Phe α351 and the bifocal interaction with Asn α329 of the α2 subunit. A significant and surprising finding is that all analyzed analogs have a *cis*-configuration at the Val-Dil amide bond while in their functionally relevant tubulin bound state, whereas in solution this bond is exclusively in the *trans*-configuration. This remarkable observation shines light onto the preferred binding mode of auristatins which is suggestive for further designs of novel analogs with pre-oriented *cis*-amide bonds in between Val and Dil. All new N-terminal modifications led to a significant increase in apparent intrinsic clearance values, a fact that could provide a safety advantage when systemic exposure needs to be minimized, i.e. for the application of these compounds as payloads in antibody drug conjugates.[22] The utility of the new auristatin analogs as ADC payloads including the development of the lead analog **20a** (PF-06380101) will be reported in due course.[47]

EXPERIMENTAL SECTION

Experiments were generally carried out under inert atmosphere (nitrogen or argon), particularly in cases where oxygen- or moisture-sensitive reagents or intermediates were employed. Commercial solvents and reagents were typically used without further purification, including anhydrous solvents where appropriate. Amino acid **19i** and **19**j were prepared previously and the absolute stereochemistry was confirmed herein as described in the supporting information.[47] Products were dried under vacuum before being carried on to further reactions or submitted for biological testing. Compound names were generated with ACD Labs software. All compounds were >95 % purity as determined by HPLC. All flash chromatographic separations were performed using Redisep R_f gold normal phase silica columns or RediSep R_f Reversed-phase C18 columns. Preparative Reverse Phase HPLC was performed on various instruments including: *Method A*. Gilson with Phenomenex Luna C18, 100 x 30 mm, 10 μm; Flow rate 20 mL/min; Detection: DAD 210 nm, 254 nm. *Method B*. Shimadzu with Phenomenex Gemini C18, 21.2 × 250mm, 5 μm; Flow rate 35 mL/min. Detection: DAD 220 nm MS (+) range 100-1200 daltons; MS Trigger. *Method C:* Waters Sunfire C18 19x100, 5 μm; Flow rate 25 mL/min. Detection: DAD 215 nm MS (+) range 160-1000 daltons. LC-MS was obtained with UPLC/MS system Waters Acquity UPLC (Acquity Binary Solvent Manager, 2777C-Autosampler, Acquity PDA, Acquity ELS and Acquity Column Manager) and Waters Acquity SQ systems from Waters Corporation, Milford, MA utilizing: Waters Acquity UPLC BEH, C18, (2.1 x 50 mm, 1.7 μm) Mobile phase A: 0.1% formic acid in water (v/v); Mobile phase B: 0.1% formic acid in CH_3CN (v/v); Gradient: 5% B over 0.1 minute, 5% to 95% B over 0.7 minute, 95% B over 0.1 minute; Flow rate1.25 mL/minute. Temperature: 60 °C; Detection: 200-450 nm; MS (+) range 100-1200

daltons; Injection volume: 5 μL. All NMR spectra were collected on one of three instruments: 1) Bruker 500 Avance III with a 5 mm DCH Helium cryoprobe (500.13 MHz for ^{1}H; 125.77 MHz for ^{13}C), 2) Bruker 500 Avance III with a 5 mm Prodigy BBO cryoprobe (499.82 MHz for ^{1}H; 125.69 MHz for ^{13}C), 3) Bruker 400 Avance III with a 5 mm BBFO probe (399.72 MHz for ^{1}H; 100.52 MHz for ^{13}C) using DMSO-d_6 as the solvent and referencing the residual solvent peak. Accurate Mass Spectrometry analyses were conducted on an Agilent 6220 TOF mass spectrometer (Agilent Technologies, Wilmington, DE) in positive or negative electrospray mode. The system was calibrated to greater than 1 ppm accuracy across the mass range prior to analyses according to manufacturer's specifications. The samples were separated using UHPLC on an Agilent 1200 (Agilent Technologies, Wilmington, DE) system prior to mass spectrometric analysis. The resulting spectra were automatically lockmass corrected and the target mass ions and any confirming adducts (Na^+, NH_4^+) were extracted and combined as a chromatogram. The mass accuracy was calculated for all observed isotopes against the theoretical mass ions derived from the chemical formula using MassHunter software (Agilent Technologies, Wilmington, DE).

Synthesis of (2*R*,3*R*)-3-methoxy-2-methyl-*N*-[(1*S*)-2-phenyl-1-(1,3-thiazol-2-yl)ethyl]-3-[(2*S*)-pyrrolidin-2-yl]propanamide, hydrochloric acid salt. To a solution of Boc-DAP-DOE, **16**) [47,48] (5.0 g, 10.56 mmol) in dioxane (25 mL) was added a solution of 4 *N* HCl (dioxane, 10 mL). After 3h the reaction was concentrated *in vacuo* to give the deprotected product (3.9 g, 100%) as a light yellow solid, which was used in the next step without further purification. *m/z* 374.3 $[M+H]^+$

Synthesis of (3*R*,4*S*,5*S*)-4-[{*N*-[(9*H*-fluoren-9-ylmethoxy)carbonyl]-L-valyl}(methyl)amino]-3-methoxy-5-methylheptanoic acid. To a solution of Fmoc-Val-Dil-O*t*Bu **15** [47] (1.62 g, 2.79 mmol) in DCM (10 mL) was added TFA (3 mL). After 3h, the mixture was concentrated *in*

vacuo to give the deprotected acid (1.42 g, 97%), which was used in the next step without further purification. *m/z* 525.3 $[M+H]^+$.

Synthesis of *N~2~-[(1-aminocyclopentyl)carbonyl]-N-[(3R,4S,5S)-3-methoxy-1-{(2S)-2-[(1R,2R)-1-methoxy-2-methyl-3-oxo-3-{[(1S)-2-phenyl-1-(1,3-thiazol-2-yl)ethyl]amino}propyl]pyrrolidin-1-yl}-5-methyl-1-oxoheptan-4-yl]-N-methyl-L-valinamide* (**17**). To a solution of Fmoc-Val-Dil-OH (5.48 g, 10.1 mmol) and DAP-DOE (3.90 g, 10.1 mmol) in DCM (50 ml) was added HATU (4.91 g, 12.5 mmol) and *N*,*N*-Diisopropylethylamine (5.51 mL, 31.3 mmol). After stirring at rt overnight, the mixture was concentrated *in vacuo* and redissolved in EtOAc (100 ml). The organic layer was washed with 1 *N* HCl (2 x 30 mL) and brine (30 mL). The organic solution was dried over Na_2SO_4 and the solvent decanted and removed *in vacuo.* The crude oil was purified by silica gel chromatography (0% to 50% acetone in heptane) to give the desired product (7.2 g, 78%) as a white solid. ^{1}H NMR (500 MHz, DMSO-d_6 presumed to be a mixture of *cis/trans* rotamers) δ [8.83 (d, *J* = 8.7 Hz) and 8.60 (d, *J* = 8.4 Hz), 1H], 7.88 (d, *J* = 7.6 Hz, 2H), [7.78 (d, *J* = 3.2 Hz) and 7.76 (d, *J* = 3.3 Hz), 1H], 7.71 (d, *J* = 7.4 Hz, 2H), [7.64 (d, *J* = 3.2 Hz) and 7.61 (d, *J* = 3.2 Hz), 1H], 7.56 – 7.11 (m, 10H), [5.51 (ddd, *J* = 12.5, 8.7, and 4.1 Hz) and 5.39 (ddd, *J* = 11.1, 8.3, and 4.3 Hz), 1H], 4.38 – 4.12 (m, 3H), 3.98 (d, *J* = 8.2 Hz, 2H), 3.82 – 3.30 (m, 8H), [3.24 (s) and 3.19 (s), 3H], [3.21 (s) and 3.17 (s), 3H], 3.03 (s) and 2.95 (s), 3H], 2.44 – 1.13 (m, 16H), [1.09 (d, *J* = 6.6 Hz) and 1.05 (d, *J* = 6.7 Hz), 3H], 0.97 – 0.83 (m, 9H), 0.72 (t, *J* = 7.5Hz, 3H). ^{13}C NMR (126 MHz, DMSO-d_6) δ 173.83, 173.57, 173.55, 173.16, 169.42, 169.08, 156.68, 144.36, 144.33, 144.20, 143.03, 142.84, 141.16, 141.13, 138.30, 138.12, 129.43, 129.14, 128.52, 128.08, 127.50, 127.46, 126.78, 126.63, 125.90, 125.86, 125.73, 120.52, 120.39, 120.29, 85.53, 81.63, 77.99, 66.22, 61.42, 60.68, 58.95, 58.65, 57.67, 57.54, 56.86, 56.74, 55.36, 52.14, 51.21, 47.56, 47.14, 46.62, 43.88, 43.59, 37.75,

35.61, 32.79, 32.18, 31.72, 30.27, 28.82, 25.79, 25.62, 24.79, 24.70, 23.62, 22.56, 19.58, 19.29, 18.92, 18.67, 16.61, 16.19, 15.94, 15.66, 15.40, 14.41, 10.98, and 10.72. LC-MS: *m/z* 881.3 $[M+H]^+$, 903.3 $[M+Na]^+$.

Synthesis of *N*-[(3*R*,4*S*,5*S*)-3-methoxy-1-{(2*S*)-2-[(1*R*,2*R*)-1-methoxy-2-methyl-3-oxo-3-{[(1*S*)-2-phenyl-1-(1,3-thiazol-2-yl)ethyl]amino}propyl]pyrrolidin-1-yl}-5-methyl-1-oxoheptan-4-yl]-*N*-methyl-L-valinamide (**18**). Tetramer **17** (5.00 g, 5.68 mmol) was dissolved in THF (10 mL) and diethylamine (3 mL) and the reaction mixture was stirred for 3h at rt. The solvent was removed and the crude material was purified by silica gel chromatography (0% to 10% MeOH in DCM) to give the desired compound (2.952 g, 79%) as a solid.

^{1}H NMR (500 MHz, DMSO-d_6 presumed to be a mixture of *cis/trans* rotamers) δ [8.82 (d, *J* = 8.7 Hz) and 8.60 (d, *J* = 8.4 Hz),1H], [7.79 (d, *J* = 3.3 Hz) and 7.76 (d, *J* = 3.2 Hz), 1H], [7.64 (d, *J* = 3.3 Hz) and 7.61 (d, *J* = 3.3 Hz), 1H], 7.31 – 7.11 (m, 5H), [5.53 (ddd, *J* = 12.5, 8.7, and 4.2 Hz) and 5.39 (ddd, *J* = 11.0, 8.4, and 4.3 Hz), 1H], 4.02 – 3.93 (m, 1H), 3.83 – 2.95 (m, 11H), [3.25 (s) and 3.19 (s), 3H], [3.19 (s) and 3.15 (s), 3H], [2.94 (s) and 2.84 (s), 3H], 2.42 – 0.74 (m, 23H); ^{13}C NMR (126 MHz, DMSO-d_6) δ 177.50, 177.36, 176.54, 176.50, 173.84, 173.73, 173.60, 173.58, 173.55, 173.27, 173.00, 170.76, 169.55, 169.30, 169.13, 168.95, 143.08, 143.00, 142.84, 138.32, 138.17, 138.03, 129.44, 129.39, 129.02, 128.61, 128.54, 128.51, 126.79, 126.74, 126.67, 126.60, 120.43, 120.37, 120.29, 85.63, 85.55, 81.74, 81.65, 79.20, 78.17, 77.87, 63.04, 62.99, 61.45, 61.42, 60.73, 60.70, 60.20, 58.95, 58.69, 57.96, 57.82, 57.70, 57.53, 56.21, 56.09, 55.82, 55.64, 55.36, 52.14, 51.80, 51.00, 47.54, 47.44, 46.70, 46.59, 43.88, 43.77, 43.58, 43.53, 37.85, 37.18, 35.74, 35.59, 34.67, 34.37, 33.25, 32.43, 31.83, 31.67, 31.40, 30.35, 30.15, 26.62, 26.41, 25.99, 25.78, 25.58, 24.79, 24.70, 23.63, 22.56, 21.22, 20.76, 20.74, 20.60, 20.33,

17.90, 17.70, 17.23, 16.82, 16.38, 16.30, 16.26, 16.03, 15.66, 15.64, 15.40, 15.29, 14.56, 14.40, 12.30, 12.28, 11.36, and 10.99. LC-MS: *m/z* 658.5 $[M+H]^+$, 680.5 $[M+Na]^+$.

Synthesis of 2-methylalanyl-*N*-[(3*R*,4*S*,5*S*)-3-methoxy-1-{(2*S*)-2-[(1*R*,2*R*)-1-methoxy-2-methyl-3-oxo-3-{[(1*S*)-2-phenyl-1-(1,3-thiazol-2-yl)ethyl]amino}propyl]pyrrolidin-1-yl}-5-methyl-1-oxoheptan-4-yl]-*N*-methyl-L-valinamide (**20a**). *Step 1*. To the solution of Fmoc aminoisobutyric acid **19a** (39.7 mg, 0.122 mmol) and tetramer **18** (80.3 mg, 0.122 mmol) in DCM (4 mL) was added HATU (71.7 mg, 0.183 mmol) and *N,N*-Diisopropylethylamine (64 µL, 0.366 mmol) and the solution was stirred at rt overnight. The solvent was removed and the crude residue dissolved in EtOAc (6 mL), washed with 1 *N* HCl (2 x 2 mL) and brine, and dried over Na_2SO_4. The solvent was removed *in vacuo* and the crude material purified by flash chromatography (0% to 50% EtOAc in heptane) to provide the protected pentamer intermediate (85 mg, 48%). *Step 2*. The protected pentamer (85 mg, 0.088 mmol) was taken up in THF (1 ml) and diethylamine (0.5 mL) was added. After stirring for 2h at rt the solvent was evaporated and the crude residue taken up in DCM (2 mL), and the solution loaded directly onto silica column and purified by flash chromatography (0% to 20% MeOH in DCM) to give the desired product (33 mg, 58%) as a white solid. ^{1}H NMR (DMSO-d_6, 500 MHz at 32 ^{o}C, presumed to be a mixture of *cis/trans* rotamers) δ [8.86 (d, *J* = 8.7 Hz) and 8.63 (d, *J* = 8.2 Hz), 1H], [8.15 (d, *J* = 9.2 Hz) and 8.12 (d, *J* = 9.1 Hz), 1H], [7.80 (d, *J* = 3.1 Hz) and 7.77 (d, *J* = 3.2 Hz), 1H], [7.66 (d, *J* = 3.2 Hz) and 7.63 (d, *J* = 3.2 Hz), 1H], 7.32 – 7.12 (5H, m), [5.52 (ddd, *J* = 12.2, 8.7, and 4.2 Hz) and 5.39 (ddd, *J* = 11.8, 8.2, and 4.3 Hz), 1H], 4.73-4.58 (m, 1H), [4.61 (t, *J* = 8.3 Hz) and 4.51 (t, *J* = 8.5 Hz), 1H], 3.99 (m, 1H), 3.82 – 2.95 (m, 7H), [3.26 (s) and 3.20 (s), 3H], [3.21 (s) and 3.17 (s), 3H], [3.03 (s) and 2.94 (s), 3H], 2.41- 0.83 (m, 28H), 0.78 (t, *J* = 7.4 Hz, 3H); ^{13}C NMR (DMSO-d_6, 126 MHz at 60 ^{o}C) δ 175.6, 175.4, 173.2, 172.9, 172.7, 172.4, 172.2,

172.1, 168.8, 168.4, 142.3, 142.0, 137.6, 137.5, 128.7, 128.5, 127.8, 127.8, 126.1, 125.9, 119.6, 119.5, 85.0, 81.2, 77.4, 77.4, 60.7, 59.9, 58.4, 58.1, 57.0, 56.9, 54.6, 54.6, 53.6, 53.5, 51.5, 50.7, 46.9, 45.9, 43.2, 42.9, 37.3, 35.2, 32.4, 31.7, 31.1, 30.1, 30.1, 27.6, 27.6, 27.1, 27.0, 25.1, 25.0, 24.1, 24.0, 22.9, 19.1, 18.8, 17.6, 17.4, 15.6, 15.3, 14.9, 14.5, 13.6, 10.3, and 10.0. HRMS *m/z* 743.4524 $[M + H]^+$. Calcd for $C_{39}H_{63}N_6O_6S$, 743.4452.

Synthesis of *N*,2-dimethylalanyl-*N*-[(3*R*,4*S*,5*S*)-3-methoxy-1-{(2*S*)-2-[(1*R*,2*R*)-1-methoxy-2-methyl-3-oxo-3-{[(1*S*)-2-phenyl-1-(1,3-thiazol-2-yl)ethyl]amino}propyl]pyrrolidin-1-yl}-5-methyl-1-oxoheptan-4-yl]-*N*-methyl-L-valinamide (**20b**). *Step 1*. To a solution of Fmoc-*N*-methyl aminoisobutyric acid **19b** (25 mg, 0.076 mmol) and tetramer **18** (50 mg, 0.076 mmol) in DCM (2 mL) was added HATU (33 mg, 0.084 mmol), followed by *N*,*N*-Diisopropylethylamine (0.04 mL, 0.228 mmol). The reaction was allowed to stir at rt for 4h, then the solvent was removed and the crude residue partitioned between EtOAc (3 mL) and 1 *N* HCl (1 mL). The layers were separated and the organic solution washed with 1 *N* HCl (1 mL) and brine (1 mL) and dried over Na_2SO_4 and evaporated. *Step 2*. The residue was taken up in THF (2 mL) and diethylamine (0.5 mL) was added. The reaction was stirred for 2h at rt, then the solvent was evaporated and the crude residue was dissolved in EtOAc (2 mL). The solution was loaded directly onto a silica gel column and purified by flash chromatography (0% to 30% MeOH in EtOAc) to give the desired product (33 mg, 58%) as a white solid. ^{1}H NMR (500 MHz, DMSO-d_6, presumed to be a mixture of *cis/trans* rotamers) δ [8.87 (d, *J* = 8.7 Hz,) and 8.64 (d, *J* = 8.4 Hz), 1H], 7.83 (d, *J* = 8.9 Hz) and 7.79 (d, *J* = 3.3 Hz) 1H], [7.77 (d, *J* = 3.3 Hz) and 7.66 (d, *J* = 3.3 Hz) 1H], [7.62 (d, *J* = 3.3 Hz) and 7.60 (d, 3.3 Hz) 1H], 7.31 – 7.11 (m, 5H), [5.52 (ddd, *J* = 12.3, 8.6, and 4.1 Hz) and 5.38 (ddd, *J* = 11.4, 8.4, and 4.2 Hz) 1H], [4.71 (m) and 4.60 (m), 1H], [4.60 (dd, *J* = 9.3 and 7.3 Hz) and 4.50 (dd, *J* = 9.3 and 8.0 Hz), 1H], 4.01 –

3.94 (m, 1H), 3.80-2.90 (m, 5H), [3.25 (s) and 3.20 (s), 3H], [3.19 (s) and 3.15 (s), 3H], 3.03 (s) and 2.94 (s), 3H], 2.45-1.92 (m, 6H), 2.10 (s) and 2.09 (s), 3H], 1.85 – 1.20 (m, 10H), [1.15 (s) and 1.08 (s), 3H], [1.10 (d, J = 6.7 Hz,) and 1.05 (d, J = 6.8 Hz), 3H], 0.93-0.83 (m, 6H), 0.75 (t, J = 7.2 Hz, 3H); ^{13}C NMR (126 MHz, DMSO-d_6) δ 176.21, 176.14, 173.86, 173.58, 173.56, 173.21, 173.16, 173.13, 169.43, 169.06, 143.05, 142.85, 138.31, 138.11, 129.44, 129.11, 128.53, 126.79, 126.64, 120.40, 120.29, 85.53, 81.61, 77.91, 61.43, 60.69, 59.00, 58.96, 58.67, 57.68, 57.56, 55.54, 54.03, 53.83, 47.57, 46.61, 43.89, 43.60, 37.70, 35.55, 32.59, 31.97, 31.69, 30.93, 30.88, 30.11, 25.80, 25.75, 25.70, 25.60, 24.87, 24.79, 24.77, 24.71, 23.63, 19.77, 19.46, 18.51, 18.25, 16.12, 15.88, 15.66, 15.41, 10.83, and 10.53. HRMS *m/z* 757.4698 $[M + H]^+$. Calcd for $C_{40}H_{66}N_6O_6S$, 757.4681.

Synthesis of *N ~2~* -[(1-aminocyclopropyl)carbonyl]-*N*-[(3*R*,4*S*,5*S*)-3-methoxy-1-{(2*S*)-2-[(1*R*,2*R*)-1-methoxy-2-methyl-3-oxo-3-{[(1*S*)-2-phenyl-1-(1,3-thiazol-2-yl)ethyl]amino}propyl] pyrrolidin-1-yl}-5-methyl-1-oxoheptan-4-yl]-*N*-methyl-L-valinamide (**20c**). *Step 1*. To a solution 1-Fmoc-amino cyclopropane carboxylic acid **19c** (98.3 mg, 0.304 mmol) in DCM (15 mL) at 0 °C was added HATU (120 mg, 0.334 mmol) and *N*,*N*-Diisopropylethylamine (0.1 mL, 0.608 mmol). The solution was stirred for 15 min and tetramer **18** (0.2 g, 0.304 mmol) was added. The reaction was stirred at rt for 1h then the solution was concentrated *in vacuo*. The residue was purified by flash column chromatography (10% to 90% DCM in EtOAc) to give the protected pentamer (155 mg, 52.9%) as a white solid. *Step 2*. The protected pentamer (40 mg, 0.042 mmol) was dissolved in THF (1 mL), diethylamine (0.5 mL) was added, and the reaction was stirred at rt overnight. The solvent was removed and the crude residue re-dissolved in EtOAc (2 mL), loaded directly onto a silica gel column, and purified by flash chromatography (0% to 30% MeOH in EtOAc) to afford the desired compound (26.7 mg, 86%) as a white solid.

^{1}H NMR (400 MHz, DMSO-d_6) δ [8.85 (d, J = 8.7 Hz) and 8.62 (d, J = 8.4 Hz), 1H], [8.21 (d, J = 9.2 Hz) and 8.15 (d, J = 9.2 Hz), 1H], [7.78 (dd, J = 8.3 and 3.3 Hz) and 7.63 (dd, J = 10.5 and 3.2 Hz), 1H] 7.32 – 7.12 (m, 5H), [5.53 (ddd, J = 12.4, 8.6 and 4.1 Hz) and 5.39 (ddd, J = 12.1, 8.3, and 4.1 Hz), 1H], 4.70 (m, 1H), [4.66 (dd, J = 9.2 and 5.8 Hz) and 4.55 (dd, J = 9.1 and 6.8 Hz), 1H], 3.98 (d, J = 7.0 Hz, 1H), 3.83 – 2.87 (m, 6H), [3.25 (s) and 3.19 (s), 3H], [3.21 (s) and 3.16 (s), 3H], [3.03 (s) and 2.92 (s), 3H], 2.45 – 0.64 (m, 29H); ^{13}C NMR (126 MHz, DMSO-d_6) δ 175.13, 175.08, 173.89, 173.58, 173.55, 173.19, 173.03, 172.94, 169.46, 169.07, 143.05, 142.84, 138.30, 138.08, 129.44, 129.04, 128.53, 126.80, 126.64, 120.39, 120.29, 85.51, 81.80, 81.63, 78.05, 77.95, 61.42, 61.40, 60.68, 58.96, 58.71, 58.12, 57.73, 57.57, 55.86, 54.33, 54.09, 53.47, 52.20, 52.15, 51.01, 47.57, 46.61, 43.89, 43.79, 43.69, 43.61, 35.76, 35.72, 35.69, 35.52, 32.73, 32.07, 31.65, 31.42, 31.02, 30.99, 30.38, 29.75, 25.94, 25.89, 25.57, 24.79, 24.74, 24.71, 23.63, 20.54, 20.08, 19.66, 18.42, 18.31, 18.08, 18.04, 17.97, 17.64, 17.33, 16.38, 16.21, 15.96, 15.68, 15.61, 15.41, 15.17, 12.50, 12.24, 11.07, 10.83. HRMS *m/z* 763.4182 $[M + Na]^+$. Calcd for $C_{39}H_{60}N_6NaO_6S$, 763.4187.

Synthesis of *N*~2~-[(1-aminocyclopentyl)carbonyl]-*N*-[(3*R*,4*S*,5*S*)-3-methoxy-1-{(2*S*)-2-[(1*R*,2*R*)-1-methoxy-2-methyl-3-oxo-3-{[(1*S*)-2-phenyl-1-(1,3-thiazol-2-yl)ethyl]amino}propyl]pyrrolidin-1-yl}-5-methyl-1-oxoheptan-4-yl]-*N*-methyl-L-valinamide (**20d**). *Step 1.* To a solution of Fmoc-amino cyclopentane amino acid **19d** (106.7 mg, 0.304 mmol) in DCM (15 mL) at 0 °C was added HATU (120 mg, 0.334 mmol) and *N*,*N*-diisopropylethylamine (0.1 mL, 0.608 mmol). The solution was stirred for 15 min and tetramer **18** (0.2 g, 0.304 mmol) was added. The reaction mixture was stirred at rt for 1h then concentrated *in vacuo*. The residue was purified by flash column chromatography (10% to 90% DCM in EtOAc) to give the desired product (165 mg, 54.8%) as a white solid. *Step 2.* The

Fmoc-pentamer (40 mg, 0.40 mmol) was taken up in THF (2 mL), diethylamine (0.5 mL) was added, and the reaction was stirred at rt overnight. The solvent was removed and the crude residue dissolved in EtOAc (2 mL), loaded directly onto a silica gel column, and purified by flash chromatography (0 to 30% MeOH in EtOAc) to afford the desired compound (31 mg, 97%) as a white solid. ^{1}H NMR (400 MHz, DMSO-d_6, presumed to be a mixture of *cis/trans* rotamers) δ [8.85 (d, *J* = 8.7 Hz) and 8.62 (d, *J* = 8.4 Hz), 1H], [8.24 (d, *J* = 9.3 Hz) and 8.20 (d, *J* = 9.4 Hz), 1H], [7.79 (d, *J* = 3.3 Hz) and 7.77 (d, *J* = 3.3 H), 1H], [7.65 (d, *J* = 3.2 Hz, 1H) and 7.62 (d, *J* = 3.3 Hz), 1H], 7.33 – 7.10 (m, 5H), [5.53 (ddd, *J* = 12.5, 8.6, and 4.2 Hz) and 5.39 (ddd, *J* = 12.1, 8.4, and 4.1 Hz), 1H], 4.72-4.50 (m, 1H), [4.63 (dd, *J* = 9.3 and 6.6 Hz) and 4.53 (dd, *J* = 9.3 and 7.5 Hz), 1H], 3.80-2.90 (m, 7H), [3.25 (s) and 3.19 (s), 3H], [3.21 (s) and 3.16 (s), 3H], [3.03 (s) and 2.93 (s), 3H], 2.45-0.08 (m, 28H), [1.10 (d, *J* = 6.7 Hz) and 1.05 (d, *J* = 6.8 Hz), 3H], 0.77 (t, *J* = 7.2 Hz, 3H); ^{13}C NMR (126 MHz, DMSO-d_6) δ 177.27, 177.23, 173.87, 173.58, 173.55, 173.17, 173.08, 173.02, 169.45, 169.07, 143.05, 142.84, 138.31, 138.10, 129.44, 129.08, 128.53, 126.79, 126.64, 120.39, 120.29, 85.53, 81.63, 77.99, 65.21, 65.15, 63.34, 61.42, 60.69, 60.20, 58.96, 58.69, 58.18, 57.71, 57.56, 55.73, 55.36, 54.13, 53.92, 52.20, 52.15, 51.10, 47.57, 46.61, 43.89, 43.60, 35.55, 32.79, 32.11, 31.69, 31.00, 30.93, 30.36, 29.75, 25.87, 25.83, 25.59, 24.79, 24.72, 24.70, 24.65, 23.63, 21.22, 20.55, 19.96, 19.60, 18.26, 17.92, 17.15, 17.09, 16.32, 16.28, 16.20, 15.96, 15.67, 15.40, 15.14, 14.56, 12.49, 12.25, 11.00, 10.74; HRMS *m/z* 791.451 $[M + Na]^+$. Calcd for $C_{41}H_{64}N_6NaO_6S$, 791.450.

Synthesis of *N*~2~-(3-amino-2,2-dimethylpropanoyl)-*N*-[(3*R*,4*S*,5*S*)-3-methoxy-1-{(2*S*)-2-[(1*R*,2*R*)-1-methoxy-2-methyl-3-oxo-3-{[(1*S*)-2-phenyl-1-(1,3-thiazol-2-yl)ethyl]amino}propyl] pyrrolidin-1-yl}-5-methyl-1-oxoheptan-4-yl]-*N*-methyl-L-valinamide, trifluoroacetic acid salt (**20e**). *Step 1*. To a solution of tetramer **18** (100 mg, 0.152 mmol) in DCM (4 mL) and DMF (0.5

mL) was added 3-{[(9*H*-fluoren-9-ylmethoxy)carbonyl]amino}-2,2-dimethylpropanoic acid **19e** (51.6 mg, 0.152 mmol), followed by *N*,*N*-diisopropylethylamine (80.0 μL, 0.457 mmol) and HATU (89.8 mg, 0.229 mmol). The reaction was stirred for 18h then concentrated *in vacuo*. The residue was dissolved in EtOAc (6 mL) and washed with 1 *N* HCl and brine. The organic layer was dried over Na_2SO_4, filtered, and concentrated *in vacuo*. The residue was purified by silica gel chromatography (0% to 50% acetone in heptane) to provide the desired product (90 mg, 60%) as a white solid. *Step 2*. To this resulting Fmoc-protected pentamer (86 mg, 0.088 mmol) in THF (2 mL) was added diethylamine (10 mL). After stirring overnight, the reaction was concentrated *in vacuo* and the residue was purified by HPLC (Method A, 10% CH_3CN/90% H_2O to 100% CH_3CN/0% H_2O, both solvents containing 0.02% TFA) to give the desired product (55 mg, 72%) a white solid. ^{1}H NMR (500 MHz, DMSO-d_6) δ [8.91 (d, J = 8.7 Hz) and 8.66 (d, J = 8.4 Hz), 1H], [7.96 (d, J = 8.4 Hz) and 7.89 (d, J = 8.5 Hz), 1H], 7.80 (d, J = 3.3 Hz) and 7.77 (d, J = 3.2 Hz), 1H], [7.67 (d, J = 3.2 Hz) and 7.63 (d, J = 3.2 Hz), 1H], 7.31 – 7.12 (m, 5H), [5.48 (ddd, J = 12.5, 8.7, and 4.2 Hz) and 5.38 (ddd, J = 11.3, 8.4, and 4.2 Hz), 1H], 4.79 – 4.58 (m, 1H), [4.54 (dd, J = 8.6 Hz) and 4.44 (dd, J = 8.9 Hz,), 1H], 4.00-2.75 (m, 9H), [3.24 (s) and 3.19 (s), 3H], [3.21 (s) and 3.16 (s), 3H], [3.04 (s) and 2.95 (s), 3H], 2.45-1.15 (m, 17H), 1.16 – 0.83 (m, 12H), 0.76 (t, J = 7.8 Hz, 3H); ^{13}C NMR (126 MHz, DMSO-d_6) δ 175.89, 175.87, 173.90, 173.58, 173.55, 173.33, 173.02, 169.32, 169.04, 158.70, 158.44, 158.19, 157.93, 143.14, 142.85, 138.32, 138.08, 129.44, 129.11, 128.57, 128.52, 126.83, 126.62, 120.41, 120.30, 118.52, 116.14, 85.53, 81.62, 77.91, 77.77, 61.45, 60.70, 58.97, 58.64, 57.65, 57.53, 55.24, 55.12, 52.15, 51.34, 47.57, 47.32, 47.27, 46.63, 43.88, 43.60, 37.82, 35.58, 32.05, 31.72, 30.13, 30.07, 25.67, 25.62, 24.80, 24.68, 23.62, 23.47, 22.83, 22.74, 19.55, 19.29, 19.16, 18.99, 16.19, 15.88, 15.67, 15.45, 10.85, 10.53. HRMS *m/z* 757.4696 $[M + H]^+$. Calcd for $C_{40}H_{65}N_6O_6S$, 757.4681.

Synthesis of *N*~2~-[2,2-dimethyl-3-(methylamino)propanoyl]-*N*-{(1*S*,2*R*)-2-methoxy-4-{(2*S*)-2-[(1*R*,2*R*)-1-methoxy-2-methyl-3-oxo-3-{[(1*S*)-2-phenyl-1-(1,3-thiazol-2-yl)ethyl]amino}propyl]pyrrolidin-1-yl}-1-[(1*S*)-1-methylpropyl]-4-oxobutyl}-*N*-methyl-L-valinamide, trifluoroacetic acid salt (**20f**). *Step 1*. To a vial containing tetramer **18** (100 mg, 0.152 mmol) in DCM (1 mL) was added Boc-2,2-dimethyl-3-(methylamino)propanoic acid **19f** (36 mg, 0.152 mmol), followed by *N*,*N*-Diisopropylethylamine (0.080 mL, 0.456 mmol) and HATU (66 mg, 0.17 mmol). The reaction was stirred at rt for 1h then concentrated *in vacuo*. The residue was dissolved in EtOAc and washed with 1 *N* HCl (2x) and brine (1x). The organic layer was dried over Na_2SO_4, decanted, and concentrated *in vacuo*. *Step 2*. Dioxane (1 mL) was added, followed by a solution of 4 *N* HCl (dioxane, 1.0 mL, 4.0 mmol). The reaction was stirred at rt for 12h and concentrated *in vacuo*. The crude material was purified by HPLC (Method A, 10% CH_3CN/90% H_2O to 100% CH_3CN/0% H_2O, both solvents containing 0.02% TFA) to yield the desired product (55.8 mg, 41%) as a solid. ^{1}H NMR (400 MHz, DMSO-d_6) δ [8.92 (d, *J* = 8.8 Hz) and 8.65 (d, *J* = 8.5 Hz), 1H], 8.22 (m, 1H), [8.00 (d, *J* = 8.6 Hz) and 7.96 (d, *J* = 8.6 Hz), 1H], [7.80 (d, *J* = 3.3 Hz) and 7.77 (d, *J* = 3.3 Hz), 1H], [7.66 (d, *J* = 3.3 Hz) and 7.62 (d, *J* = 3.3 Hz), 1H], 7.33 – 7.10 (m, 5H), [5.48 (ddd, *J* = 12.4, 8.6, and 4.1 Hz) and 5.38 (ddd, *J* = 12.2, 8.4, and 4.2 Hz), 1H], 4.80-4.65 (m, 1H), [4.57 (dd, *J* = 8.6 Hz) and 4.47 (dd, *J* = 8.9 Hz), 1H], 4.00 (m, 1H), 3.81-2.85 (m, 11H), [3.24 (s) and 3.20 (s), 3H], [3.21 (s) and 3.17 (s), 3H],[3.04 (s) and 2.95 (s), 3H], 2.45-0.07 (m, 32H); ^{13}C NMR (126 MHz, DMSO-d_6) δ 175.90, 175.84, 173.92, 173.60, 173.58, 173.39, 172.87, 169.27, 169.02, 158.95, 158.67, 158.39, 158.12, 143.21, 142.89, 138.33, 138.06, 129.68, 129.45, 129.10, 128.58, 128.52, 126.86, 126.62, 120.45, 120.33, 120.13, 117.79, 115.44, 113.10, 85.48, 81.54, 77.86, 77.63, 61.46, 60.72, 58.94, 58.60, 57.65, 57.53, 57.11, 57.06, 55.44, 55.19, 55.08, 52.14, 51.31, 47.57, 46.63, 43.88, 43.60, 37.78,

35.46, 34.81, 34.79, 32.61, 32.00, 31.74, 30.17, 30.12, 25.66, 25.60, 24.80, 24.67, 23.73, 23.69, 23.63, 22.94, 22.88, 21.53, 19.53, 19.29, 19.16, 18.99, 16.14, 15.82, 15.67, 15.50, 10.83, 10.48. HRMS *m/z* 771.4857 $[M + H]^+$. Calcd for $C_{41}H_{67}N_6O_6S$, 771.4837.

Synthesis of 2-methyl-L-prolyl-*N*-[(3*R*,4*S*,5*S*)-3-methoxy-1-{(2*S*)-2-[(1*R*,2*R*)-1-methoxy-2-methyl-3-oxo-3-{[(1*S*)-2-phenyl-1-(1,3-thiazol-2-yl)ethyl]amino}propyl]pyrrolidin-1-yl}-5-methyl-1-oxoheptan-4-yl]-*N*-methyl-L-valinamide **(20g)**. *Step 1*. To a solution of (*S*)-*N*-Boc-α-methylproline **19g** (17 mg, 0.076 mmol) and tetramer **18** (50 mg, 0.076 mmol) in DCM (2 mL) was added HATU (33 mg, 0.084 mmol) and *N*,*N*-Diisopropylethylamine (0.04 mL, 0.228 mmol). The reaction was stirred at rt for 4h. The solvent was removed and the crude residue was partitioned between EtOAc (3 mL) and 1 *N* HCl (1 mL) and the layers were separated. The organic layer was washed with 1 *N* HCl (1 mL) and brine (1 mL), then dried over Na_2SO_4 and evaporated. *Step 2*. The residue was dissolved in DCM (2 mL), TFA (0.5 mL) was added, and the reaction mixture was stirred at rt for 15 minutes. The solvent was evaporated and the crude residue was partitioned between EtOAc (4 mL) and saturated aq $NaHCO_3$ (2 mL), then the layers were separated. The organic solution was dried over Na_2SO_4 and loaded directly onto silica column and purified by flash chromatography (0% to 30% MeOH in EtOAc) to give the desired product (39 mg, 67%) as a white solid. ^{1}H NMR (500 MHz, DMSO-d_6) δ [8.87 (d, *J* = 8.8 Hz) and 8.64 (d, *J* = 8.4 Hz), 1H], [8.29 (d, *J* = 9.5 Hz) and 8.24 (d, *J* = 9.6 Hz) 1H], [7.79 (d, *J* = 3.3 Hz) and 7.77 (d, *J* = 3.3 Hz), 1H], [7.66 (d, *J* = 3.2 Hz) and 7.62 (d, *J* = 3.2 Hz), 1H], 7.31 – 7.10 (m, 5H), [5.53 (ddd, *J* = 12.5, 8.7, and 4.2 Hz) and 5.38 (ddd, *J* = 11.3, 8.5, and 4.2 Hz), 1H], 4.72-4.55 (m, 1H), [4.58 (dd, *J* = 9.5 and 6.6 Hz) and 4.48 (dd, *J* = 9.5 and 7.4 Hz), 1H], 3.97 (m, 1H), 3.80-2.62 (m, 8H), [3.25 (s) and 3.19 (s), 3H], [3.20 (s) and 3.15 (s), 3H],[3.02 (s) and 2.92 (s), 3H], 2.42-0.70 (m, 27H), [1.10 (d, *J* = 6.7 Hz) and 1.05 (d, *J* = 6.8 Hz), 3H], 0.77 (t, *J* =

7.4 Hz, 3H); ^{13}C NMR (126 MHz,DMSO-d_6) δ 176.32, 173.88, 173.63, 173.58, 173.55, 173.19, 172.93, 172.86, 169.43, 169.04, 143.06, 142.85, 138.31, 138.10, 129.44, 129.24, 129.08, 128.84, 128.53, 126.79, 126.64, 120.40, 120.29, 85.52, 81.61, 77.94, 66.82, 61.43, 61.40, 60.69, 58.96, 58.76, 58.68, 57.71, 57.57, 55.70, 55.37, 53.85, 53.67, 52.15, 51.11, 47.57, 46.91, 46.61, 43.89, 43.60, 37.83, 37.71, 37.68, 35.52, 32.71, 32.05, 31.69, 30.98, 30.93, 30.41, 26.30, 25.84, 25.80, 25.59, 25.05, 24.79, 24.70, 23.63, 21.51, 20.75, 20.68, 19.94, 19.60, 18.11, 17.82, 16.87, 16.75, 16.20, 16.17, 15.93, 15.67, 15.59, 15.41, 12.44, 12.26, 10.93, 10.65. HRMS *m/z* 769.4703 [M + H]$^+$. Calcd for $C_{41}H_{65}N_6O_6S$, 769.4681.

Synthesis of 2-methyl-D-prolyl-*N*-[(3*R*,4*S*,5*S*)-3-methoxy-1-{(2*S*)-2-[(1*R*,2*R*)-1-methoxy-2-methyl-3-oxo-3-{[(1*S*)-2-phenyl-1-(1,3-thiazol-2-yl)ethyl]amino}propyl]pyrrolidin-1-yl}-5-methyl-1-oxoheptan-4-yl]-*N*-methyl-L-valinamide (**20h**). *Step 1*. To a solution of (*R*)-*N*-Boc-α-methylproline **19h** (17 mg, 0.076 mmol) and tetramer **18** (50 mg, 0.076 mmol) in DCM (2 mL) was added HATU (33 mg, 0.084 mmol) and *N*,*N*-Diisopropylethylamine (0.04 mL, 0.228 mmol). The reaction was stirred at rt for 4h. The solvent was removed and the crude residue was partitioned between EtOAc (3 mL) and 1 *N* HCl (1 mL) and the layers were separated. The organic layer was washed with 1 *N* HCl (1 mL) and brine (1 mL), then dried over Na_2SO_4 and evaporated. *Step 2*. The residue was taken up in DCM (2 mL), TFA (0.5 mL) was added, and the reaction was stirred at rt for 15 minutes. The solvent was evaporated and the crude residue partitioned between EtOAc (4 mL) and saturated aq $NaHCO_3$ (2 mL), and the layers separated. The organic solution was dried over Na_2SO_4, loaded directly onto a silica column, and purified by flash chromatography (0% to 30% MeOH in EtOAc) to give the desired product (33 mg, 57%) as a white solid. ^{1}H NMR (500 MHz, DMSO-d_6) δ [8.86 (d, *J* = 8.7 Hz) and 8.64 (d, *J* = 8.5 Hz), 1H], [8.24 (d, *J* = 9.7 Hz) and 8.20 (d, *J* = 9.9 Hz), 1H], [7.79 (d, *J* = 3.2 Hz) and 7.77

(d, *J* = 3.3 Hz), 1H], [7.66 (d, *J* = 3.2 Hz) and 7.62 (d, *J* = 3.2 Hz), 1H], 7.32 – 7.10 (m, 5H), [5.52 (ddd, *J* = 12.3, 8.6, and 4.2 Hz) and 5.38 (ddd, *J* = 11.4, 8.4 and 4.2 Hz), 1H], 4.69 (d, *J* = 10.6 Hz, 1H), [4.55 (dd, *J* = 9.7 and 7.4 Hz) and 4.46 (dd, *J* = 9.7 and 8.0 Hz), 1H], 3.97 (m, 1H), 3.80-2.62 (m, 8), [3.24 (s) and 3.19 (s), 3H], [3.20 (s) and 3.15 (s), 3H], [3.00 (s) and 2.91 (s), 3H], 2.42-0.70 (m, 27H), [1.09 (d, *J* = 6.7 Hz) and 1.05 (d, *J* = 6.8 Hz), 3H], 0.75 (t, *J* = 7.4, 3H); ^{13}C NMR (126 MHz, DMSO-d_6) δ 176.58, 173.86, 173.58, 173.56, 173.15, 173.03, 170.77, 169.41, 169.05, 143.05, 142.85, 138.31, 138.11, 129.44, 129.11, 128.83, 128.54, 126.79, 126.64, 120.40, 120.29, 85.53, 81.61, 77.87, 66.84, 66.79, 61.42, 60.69, 60.21, 58.96, 58.67, 57.68, 57.54, 55.55, 53.83, 53.68, 52.15, 51.16, 47.57, 46.61, 46.57, 43.89, 43.60, 37.67, 37.42, 37.27, 35.53, 34.85, 32.63, 32.03, 31.69, 31.08, 31.05, 26.07, 25.74, 25.59, 24.79, 24.71, 23.63, 21.23, 19.67, 19.40, 18.29, 18.09, 16.86, 16.08, 15.86, 15.66, 15.56, 15.41, 14.56, 12.48, 10.82, 10.53. HRMS *m/z* 769.4685 $[M + H]^+$. Calcd for $C_{41}H_{65}N_6O_6S$, 769.4681.

Synthesis of N~2~-{[(3S)-3-fluoropyrrolidin-3-yl]carbonyl}-N-[(3R,4S,5S)-3-methoxy-1-{(2S)-2-[(1R,2R)-1-methoxy-2-methyl-3-oxo-3-{[(1S)-2-phenyl-1-(1,3-thiazol-2-yl)ethyl]amino}propyl]pyrrolidin-1-yl}-5-methyl-1-oxoheptan-4-yl]-N-methyl-L-valinamide, trifluoroacetic acid salt (**20i**). *Step 1*. To a solution of tetramer **18** (300 mg, 0.45 mmol) and (3*S*)-1-(*tert*-butoxycarbonyl)-3-fluoropyrrolidine-3-carboxylic acid (**19i**, see supporting information) (106 mg, 0.45 mmol) in DCM (10 mL) was added HATU (194 mg, 0.54 mmol) and *N*,*N*-Diisopropylethylamine (117 mg, 0.9 mmol) and the reaction was stirred at rt for 3h. The solvent was removed and the crude residue was purified by preparative HPLC (Method B, 55% H_2O/45% CH_3CN to 15% H_2O/85% CH_3CN, both solvents containing 0.225% NH_4OH) to afford the desired product (149 mg, 37%) as a white solid. *Step 2*. The resulting Boc-protected pentamer (20 mg, 0.02 mmol) was dissolved in DCM (0.3 mL) and CH_3CN (0.3 mL) and a

solution of 4 *N* HCl (dioxane, 0.26 mL) was added. The reaction was stirred at rt for 2.5h, the solvent was removed, and the crude material was purified by HPLC (Method C, 85% H_2O/15% CH_3CN to 50% H_2O/50% CH_3CN, both solvents containing 0.05% TFA) to obtain the desired product (18.6 mg, 91%). ^{1}H NMR (400 MHz, DMSO-d_6, presumed to be a mixture of *cis/trans* isomers) δ [9.40 (br s) and 9.23 (br s), 1H)], [8.89 (d, *J* = 8.8 Hz) and 8.65 (d, *J* = 8.4 Hz), 1H], [8.48- 8.29 (m, 1H)], [7.81 (d, *J* = 3.2 Hz) and 7.79 (d, *J* = 3.2 Hz), 1H], [7.68 (d, *J* = 3.2 Hz) and 7.65 (d, *J* = 3.6 Hz), 1H], 7.81-7.17 (m, 5H), [5.53 (ddd, *J* = 12.8, 9.2, and 4.8 Hz) and 5.41 (ddd, *J* = 12.4, 8.0, and 4.0 Hz), 1H], 4.70 (bs, 1H), [4.61 (t, *J* = 8.0 Hz) and 4.51 (t, *J* = 8.5 Hz), 1H], 3.97 (m, 1H), 3.82 – 2.85 (m, 10H), [3.25 (s) and 3.20 (s) 3H], [3.21 (s) and 3.16 (s), 3H], [3.05 (s) and 2.97 (s), 3H)], 2.40 – 0.83 (m, 25H), 0.76 (t, *J* = 7.3 Hz, 3H).; ^{13}C NMR (126 MHz, DMSO-d_6): δ 173.91, 173.58, 173.55, 173.27, 172.42, 172.29, 169.35, 169.01, 166.94, 166.91, 166.75, 166.72, 159.02, 158.74, 158.45, 158.17, 143.07, 142.85, 138.31, 138.10, 129.44, 129.12, 128.54, 128.52, 126.81, 126.63, 120.41, 120.30, 119.82, 117.49, 115.16, 112.83, 102.09, 102.02, 100.53, 85.53, 81.61, 77.89, 61.44, 60.68, 58.96, 58.66, 57.68, 57.55, 55.46, 55.27, 53.64, 53.43, 53.37, 52.14, 51.23, 47.57, 46.62, 44.89, 44.87, 43.88, 43.60, 37.69, 35.54, 35.52, 35.34, 30.16, 30.04, 25.70, 25.59, 24.80, 24.68, 23.62, 19.56, 19.16, 18.87, 18.53, 16.16, 15.91, 15.67, 15.44, 10.76, 10.52. HRMS *m/z* 773.4444 $[M + H]^+$. Calcd for $C_{40}H_{62}FN_6O_6S$, 773.4430.

Synthesis of N~2~-{[(3R)-3-fluoropyrrolidin-3-yl]carbonyl}-N-[(3R,4S,5S)-3-methoxy-1-{(2S)-2-[(1R,2R)-1-methoxy-2-methyl-3-oxo-3-{[(1S)-2-phenyl-1-(1,3-thiazol-2-yl)ethyl]amino}propyl]pyrrolidin-1-yl}-5-methyl-1-oxoheptan-4-yl]-N-methyl-L-valinamide, trifluoroacetic acid salt (**20j**). *Step 1*. To a solution of tetramer **18** (300 mg, 0.45 mmol) and (3*R*)-1-(*tert*-butoxycarbonyl)-3-fluoropyrrolidine-3-carboxylic acid (**19j**, see supporting information) (106 mg, 0.45 mmol) in DCM (10 mL) was added HATU (194 mg, 0.54 mmol) and

N,*N*-Diisopropylethylamine (117 mg, 0.9 mmol) and the reaction was stirred at rt for 3h. The solvent was removed and the crude residue was purified by HPLC (Method B, 55% H_2O/45% CH_3CN to 15% H_2O/85% CH_3CN, both solvents containing 0.225% NH_4OH) to afford the desired product (159 mg, 40%) as a white solid. *Step 2*. The resulting pentamer (25 mg, 0.03 mmol) was dissolved in CH_3CN (0.5 mL) and a solution of 4 *N* HCl (dioxane, 0.34 mL) was added. The reaction was stirred at rt for 2.5 h. The solvent was removed and the crude material was purified by HPLC (Method C, 95% H_2O/5% CH_3CN to 40% H_2O/60% CH_3CN, both solvents containing 0.05% TFA) to provide the desired product (17.7 mg, 69%). ^{1}H NMR (400 MHz, DMSO-d_6, presumed to be a mixture of *cis/trans* isomers): δ [9.33 (br s) and 9.22 (br s), 1H)], [8.88 (d, J = 8.7 Hz) and 8.63 (d, J = 8.3 Hz), 1H], [8.38 (d, J = 8.2 Hz and 8.22 (d, J = 8.2 Hz), 1H)], [7.79 (d, J = 3.3 Hz) and 7.77 (d, J = 3.3 Hz), 1H], [7.65 (d, J = 3.3 Hz) and 7.62 (d, J = 3.3 Hz), 1H], 7.30-7.12 (m, 5H), [5.51 (ddd, J = 12.8, 9.2, and 4.8 Hz) and 5.38 (ddd, J = 12.4, 8.0, and 4.0 Hz), 1H], 4.70 (bs, 1H), [4.65 (t, J = 7.8 Hz) and 4.54 (t, J = 8.3 Hz), 1H], 3.99 (m, 1H), 3.82 – 2.85 (m, 10H), [3.25 (s) and 3.20 (s) 3H], [3.21 (s) and 3.16 (s), 3H], [3.05 (s) and 2.96 (s), 3H)], 2.40 – 0.83 (m, 25H), 0.76 (t, J = 7.3 Hz, 3H).; ^{13}C NMR (126 MHz, DMSO-d_6) δ 173.92, 173.61, 173.58, 173.55, 173.27, 172.20, 169.36, 169.01, 166.88, 166.69, 143.08, 142.85, 138.31, 138.10, 129.44, 129.10, 128.54, 126.81, 126.63, 120.40, 120.30, 102.19, 102.10, 100.64, 100.55, 85.52, 81.61, 77.93, 61.44, 60.69, 58.97, 58.67, 57.70, 57.56, 55.30, 55.06, 53.53, 53.31, 52.15, 51.19, 47.58, 46.63, 44.96, 43.88, 43.61, 37.65, 35.75, 35.63, 35.56, 35.45, 30.32, 30.19, 25.78, 25.59, 24.79, 24.68, 23.62, 19.69, 19.27, 18.62, 18.22, 16.18, 15.92, 15.68, 15.45, 10.84, 10.62; HRMS *m/z* 773.4428 $[M + H]^+$. Calcd for $C_{40}H_{62}FN_6O_6S$, 773.4430.

Synthesis of (2S)-N-[(2S)-1-{[(3R,4S,5S)-3-methoxy-1-{(2S)-2-[(1R,2R)-1-methoxy-2-methyl-3-oxo-3-{[(1S)-2-phenyl-1-(1,3-thiazol-2-yl)ethyl]amino}propyl]pyrrolidin-1-yl}-5-

methyl-1-oxoheptan-4-yl](methyl)amino}-3-methyl-1-oxobutan-2-yl]-2-methylpiperidine-2-carboxamide, trifluoroacetic acid salt (**20k**). *Step 1*. To a solution of tetramer **18** (400 mg, 0.6 mmol) and (2*S*)-1-(*tert*-butoxycarbonyl)-2-methylpiperidine-2-carboxylic acid (**19k**, see supporting information) (146 mg, 0.6 mmol) in DCM (10 mL) was added HATU (259 mg, 0.72 mmol) and *N*,*N*-Diisopropylethylamine (158 mg, 1.2 mmol) and the reaction was stirred at rt for 3h. The solvent was removed and the crude residue was purified by flash silica gel chromatography (1% to 5% MeOH in DCM) to afford the desired product (200 mg, 38%) as a white solid. *Step 2*. The resulting pentamer (20 mg, 0.022 mmol) was dissolved in DCM (0.1 mL) and CH_3CN (0.1 mL) and to this solution was added a solution of 4 *N* HCl (dioxane 0.26 mL). The reaction was stirred for 2.5h at rt. The solvent was removed and the crude material was purified by HPLC (Method C, 90% H_2O/10% CH_3CN to 40% H_2O/60% CH_3CN, both solvents containing 0.05% TFA) to obtain the desired product (13.2 mg, 73%). ^{1}H NMR (400 MHz, DMSO-d_6, presumed to be a mixture of *cis/trans* isomers) δ [8.90 (d, *J* = 8.7 Hz) and 8.64 (d, *J* = 8.3 Hz), 1H], [8.85-8.65 (m), 1H)], [8.56 (d, *J* = 8.2 Hz and 8.53 (d, *J* = 8.2 Hz), 1H)], [7.80 (d, *J* = 3.3 Hz) and 7.77 (d, *J* = 3.3 Hz), 1H], [7.66 (d, *J* = 3.3 Hz) and 7.62 (d, *J* = 3.3 Hz), 1H], 7.33-7.12 (m, 5H), [5.48 (ddd, *J* = 12.8, 9.2, and 4.8 Hz) and 5.38 (ddd, *J* = 12.4, 8.0, and 4.0 Hz), 1H], 4.75 (m, 1H), [4.60 (t, *J* = 7.8 Hz) and 4.52 (t, *J* = 8.3 Hz), 1H], 3.99 (m, 1H), 3.82 – 2.90 (m, 8H), [3.25 (s) and 3.20 (s) 3H], [3.22 (s) and 3.17 (s), 3H], [3.07 (s) and 3.00 (s), 3H)], 2.45 – 0.83 (m, 29H), 0.76 (m, 3H); ^{13}C NMR (126 MHz, DMSO-d_6) δ 173.92, 173.58, 173.55, 173.31, 172.64, 170.73, 169.29, 169.00, 158.61, 158.33, 143.13, 142.86, 138.33, 138.12, 129.45, 129.17, 128.57, 128.52, 126.83, 126.62, 120.44, 120.30, 117.82, 115.48, 85.59, 81.63, 77.71, 61.46, 61.19, 61.16, 60.70, 58.97, 58.61, 57.63, 57.56, 55.59, 55.55, 52.15, 51.44, 47.58, 46.64, 43.88, 43.61, 37.79, 35.58, 32.51, 31.91, 31.74, 31.36, 30.16, 25.67, 25.62, 24.80, 24.68,

23.62, 22.36, 21.62, 19.39, 19.33, 19.25, 19.23, 18.97, 16.12, 15.80, 15.67, 15.45, 10.69, 10.35. HRMS *m/z* 783.4834 $[M + H]^+$. Calcd for $C_{42}H_{67}N_6O_6S$, 783.4837.

Synthesis of (2R)-N-[(2S)-1-{[(3R,4S,5S)-3-methoxy-1-{(2S)-2-[(1R,2R)-1-methoxy-2-methyl-3-oxo-3-{[(1S)-2-phenyl-1-(1,3-thiazol-2-yl)ethyl]amino}propyl]pyrrolidin-1-yl}-5-methyl-1-oxoheptan-4-yl](methyl)amino}-3-methyl-1-oxobutan-2-yl]-2-methylpiperidine-2-carboxamide, trifluoroacetic acid salt (**20l**). *Step 1*. To a solution of tetramer **18** (280 mg, 0.4 mmol) and (2*R*)-1-(*tert*-butoxycarbonyl)-2-methylpiperidine-2-carboxylic acid (**19l**, see supporting information) (100 mg, 0.4 mmol) in DCM (5 mL) was added HATU (182 mg, 0.48 mmol) and *N*,*N*-Diisopropylethylamine (100 mg, 0.8 mmol) and the reaction was stirred at rt for 3h. The solvent was removed and the crude residue was purified by flash silica gel chromatography (1% to 5% MeOH in DCM) to afford the desired product (220 mg, 62%) as a white solid. *Step 2*. The resulting pentamer (20 mg, 0.022 mmol) was dissolved in DCM (0.1 mL) and CH_3CN (0.1 mL) and to this solution was added a solution of 4 *N* HCl (dioxane, 0.26 mL). The reaction was stirred for 2.5 h at rt. The solvent was removed and the crude material was purified by preparative HPLC (Method C, 85% H_2O/15% CH_3CN to 45% H_2O/55% CH_3CN, both solvents containing 0.05% TFA) to obtain the desired product (11.6 mg, 61%). ^{1}H NMR (400 MHz, DMSO-d_6, presumed to be a mixture of *cis/trans* isomers) δ [8.90 (d, *J* = 8.8 Hz) and 8.64 (d, *J* = 8.3 Hz), 1H], [8.75-8.65 (m), 1H)], [8.45 (d, *J* = 8.2 Hz and 8.43 (d, *J* = 8.2 Hz), 1H)], [7.80 (d, *J* = 3.3 Hz) and 7.77 (d, *J* = 3.3 Hz), 1H], [7.66 (d, *J* = 3.3 Hz) and 7.62 (d, *J* = 3.3 Hz), 1H], 7.33-7.10 (m, 5H), [5.47 (ddd, *J* = 12.4, 8.5, and 4.2 Hz) and 5.38 (ddd, *J* = 12.1, 8.4, and 4.2 Hz), 1H], 4.73 (m, 1H), [4.58 (t, *J* = 8.8 Hz) and 4.51 (t, *J* = 8.9 Hz), 1H], 3.98 (m, 1H), 3.82 – 2.85 (m, 8H), [3.25 (s) and 3.20 (s) 3H], [3.21 (s) and 3.16 (s), 3H], [3.05 (s) and 2.99 (s), 3H)], 2.45 – 0.83 (m, 29H), 0.80-0.72 (m, 3H); ^{13}C NMR (126 MHz, DMSO-d_6) δ

173.92, 173.58, 173.55, 173.25, 172.64, 170.58, 170.55, 169.29, 169.02, 158.90, 158.62, 158.35, 158.07, 143.09, 142.85, 138.32, 138.12, 129.44, 129.18, 128.56, 128.52, 126.83, 126.62, 120.42, 120.30, 117.80, 115.45, 113.11, 85.61, 81.61, 77.99, 77.73, 61.47, 61.34, 61.33, 60.69, 58.97, 58.64, 57.63, 57.53, 55.67, 55.62, 52.15, 51.46, 47.58, 46.62, 43.89, 43.58, 41.33, 37.72, 35.56, 32.56, 32.08, 31.68, 30.21, 25.78, 25.74, 25.62, 24.80, 24.68, 23.62, 23.33, 21.68, 19.31, 19.24, 19.21, 19.18, 18.91, 16.08, 15.78, 15.66, 15.46, 10.90, 10.67. HRMS *m/z* 783.4836 $[M + H]^+$. Calcd for $C_{42}H_{67}N_6O_6S$, 783.4837.

Synthesis of *N*,2-dimethylalanyl-*N*-{(1*S*,2*R*)-4-{(2*S*)-2-[(1*R*,2*R*)-3-{[(1*S*)-1-carboxy-2-phenylethyl]amino}-1-methoxy-2-methyl-3-oxopropyl]pyrrolidin-1-yl}-2-methoxy-1-[(1*S*)-1-methylpropyl]-4-oxobutyl}-*N*-methyl-L-valinamide, trifluoroacetic acid salt (**22a**). *Step 1*. To a solution of compound **19a** (500 mg, 1.56 mmol) in DMF (25 mL) were added HATU (648 mg, 1.7 mmol) and *N,N*-Diisopropylethylamine (550 mg, 4.26 mmol). A solution of compound **21** (0.9 g, 1.42 mmol) in DMF (10 mL) was added and the reaction mixture was stirred at rt overnight. The reaction solution was concentrated *in vacuo* and the residue was purified by silica gel chromatography (0% to10% EtOAc in DCM) to give the protected pentamer (0.8 g, 73%) as a white solid. *Step 2*. The protected pentamer (440 mg, 0.47 mmol) was taken up in THF (4 mL) and a solution of LiOH (28 mg, 1.17 mmol) in water (2 mL) was added. The reaction was stirred overnight at rt. The solvent was evaporated and the residue was azeotroped with heptane (3x). The resulting crude residue was purified by HPLC (Method A, 10% CH_3CN/90% H_2O to 100% CH_3CN/0% H_2O, each solvent containing 0.02% TFA) to provide the desired product (203 mg, 53%) as a white solid. ^{1}H NMR (500 MHz, DMSO-d_6, presumed to be a mixture of *cis/trans* isomers) δ 8.45 – 8.07 (m, 4H), 7.26 – 7.13 (m, 5H), 4.78 – 4.39 (m, 3H), 3.98 (q, *J* = 7.8 Hz, 1H), 3.76-2.75 (m, 5H), [3.24 (s) and 3.20 (s), 3H], [3.20 (s) and 3.18 (s),

3H], [3.04 (s) and 2.95 (s), 3H], 2.44 – 2.04 (m, 5H), 1.87-1.19 (m, 7H), [1.53 (s) and1.52 (s), 3H], [1.41 (s) and 1.39 (s), 3H], 1.08 – 0.83 (m, 12H), 0.77 (t, J = 7.4 Hz, 3H); ^{13}C NMR (126 MHz, DMSO-d_6) δ 173.98, 173.83, 173.65, 173.58, 172.44, 171.75, 171.72, 169.39, 169.07, 158.29, 158.05, 148.81, 139.89, 138.22, 137.95, 129.39, 129.10, 128.76, 128.53, 128.50, 127.70, 126.80, 126.65, 125.06, 120.17, 85.87, 81.92, 81.88, 77.90, 68.19, 61.43, 60.67, 59.00, 58.68, 57.64, 57.59, 57.06, 57.03, 55.60, 55.33, 53.46, 52.41, 47.54, 46.63, 43.56, 43.39, 41.83, 35.65, 32.74, 32.06, 31.71, 30.34, 30.31, 28.81, 25.75, 25.68, 24.77, 24.73, 23.79, 23.60, 23.58, 22.55, 19.35, 19.18, 18.92, 18.87, 16.19, 15.91, 15.68, 15.33, 14.40, 11.47, 10.81, 10.47. HRMS *m/z* 704.4591 $[M + H]^+$. Calcd for $C_{38}H_{61}N_5O_8$, 704.4593.

Synthesis of *N*,2-dimethylalanyl-*N*-{(1*S*,2*R*)-4-{(2*S*)-2-[(1*R*,2*R*)-3-{[(1*S*)-1-carboxy-2-phenylethyl]amino}-1-methoxy-2-methyl-3-oxopropyl]pyrrolidin-1-yl}-2-methoxy-1-[(1*S*)-1-methylpropyl]-4-oxobutyl}-*N*-methyl-L-valinamide, trifluoroacetic acid salt (**22b**). *Step 1*. To a solution of Fmoc-*N*-methyl aminoisobutyric acid **19b** (36 mg, 0.106 mmol) and tetramer **21** (60.8 mg, 0.096 mmol) in DCM (2 mL) was added HATU (45 mg, 0.115 mmol), followed by *N*,*N*-Diisopropylethylamine (0.05 mL, 0.288 mmol). The reaction was stirred at rt for 4h, then the solvent was removed and the crude residue partitioned between EtOAc (3 mL) and 1 *N* HCl (1 mL). The layers were separated and the organic layer washed with 1 *N* HCl (1 mL) and brine (1 mL). The resulting solution was dried over Na_2SO_4 and concentrated *in vacuo*. *Step 2*. The residue was taken up in THF (1 ml) and aq 1 *M* LiOH (0.2 mL) was added. The reaction was stirred for 4h at rt then the solvent was evaporated and the crude residue was dissolved in DMSO (1 mL). The solution was loaded directly onto an Isco C18 silica column and purified by reverse phase chromatography (0% CH_3CN/100% H_2O to 100% CH_3CN/0% H_2O, each solvent containing 0.02% TFA) to give the desired product (23 mg, 33%) as a white solid. ^{1}H NMR

(400 MHz, DMSO-d_6, presumed to be a mixture of *cis/trans* isomers) δ 8.87 (d, *J* = 9.0 Hz, 2H), [8.46 (d, *J* = 5.7 Hz) and 8.44 (d, *J* = 5.7 Hz), 1H], [8.39 (d, *J* = 8.6 Hz) and 8.13 (d, *J* = 8.2 Hz), 1H], 7.28 – 7.11 (m, 5H), 4.78 – 4.37 (m, 3H), 3.98 (m, 1H), 3.76-2.75 (m, 5H), [3.24 (s) and 3.19 (s), 3H], [3.19 (s) and 3.17 (s), 3H], [3.05 (s) and 2.96 (s), 3H], [2.46 (s) and 2.45 (s), 3H], 2.47-2.05 (m, 5H), 1.87-1.19 (m, 7H), [1.53 (s) and 1.51 (s), 3H], [1.42 (s) and 1.40 (s), 3H], 1.08 – 0.82 (m, 12H), 0.77 (d, *J* = 7.5 Hz, 3H); ^{13}C NMR (126 MHz, DMSO-d_6) δ 173.98, 173.83, 173.65, 173.59, 172.51, 171.10, 171.08, 169.37, 169.07, 138.21, 137.96, 129.39, 129.12, 128.53, 128.51, 126.80, 126.65, 85.87, 81.90, 77.92, 61.73, 61.70, 61.43, 60.66, 59.00, 58.68, 57.63, 57.57, 55.57, 53.46, 52.44, 47.55, 46.62, 43.56, 43.39, 37.75, 36.96, 36.87, 35.63, 32.61, 32.00, 31.74, 30.18, 27.71, 25.71, 24.77, 24.73, 23.58, 21.41, 21.34, 19.25, 19.08, 19.04, 19.01, 16.16, 15.90, 15.68, 15.34, 10.78, 10.48. HRMS *m/z* 718.4748 $[M + H]^+$. Calcd for $C38H_{63}N_5O_8$, 718.4749.

Synthesis of 2-methyl-L-prolyl-*N*-[(3*R*,4*S*,5*S*)-3-methoxy-1-{(2*S*)-2-[(1*R*,2*R*)-1-methoxy-2-methyl-3-oxo-3-{[(1*S*)-2-phenyl-1-(1,3-thiazol-2-yl)ethyl]amino}propyl]pyrrolidin-1-yl}-5-methyl-1-oxoheptan-4-yl]-*N*-methyl-L-valinamide (**22g**). *Step 1*. To a solution of (*S*)-*N*-Boc-α-methylproline **19g** (443 mg, 1.93 mmol) and tetramer **21** (1.02 mg, 1.61 mmol) in DCM (12 mL) was added HATU (735 mg, 1.93 mmol) and *N*,*N*-Diisopropylethylamine (1.12 mL, 6.45 mmol). The reaction was stirred at rt for 2h. The solvent was removed *in vacuo* and the crude residue was partitioned between EtOAc (30 mL) and 0.5 *N* HCl (10 mL) and the layers were separated. The organic layer was washed with brine (1 mL), then dried over Na_2SO_4 and concentrated. The crude residue was purified by flash chromatography (0% to 50% Acetone in heptane) provided the protected pentamer (1.02 g, 75%). *Step 2*. The protected pentamer (493 mg, 0.515 mmol) was dissolved in THF (4 mL) and a solution of LiOH (24.7 mg, 1.03 mmol) in

water (2 mL) was added. The reaction was stirred for 1h then the solvent was removed *in vacuo*. The crude residue was dissolved in DCM (7 mL), TFA (3 mL) was added, the reaction mixture was stirred at rt for 0.5h. The solvent was evaporated and the crude residue purified by C18 flash chromatography (0% CH_3CN/100% H_2O to 100% CH_3CN/0% H_2O, each solvent containing 0.02% TFA) to yield the desired product (325 mg, 75%) as a white solid. ^{1}H NMR (400 MHz, DMSO-d_6, presumed to be a mixture of *cis/trans* isomers) δ 9.15 – 8.68 (m, 2H), [8.39 (d, J = 8.6 Hz) and 8.13 (d, J = 8.2 Hz, 1H], 7.28 – 7.11 (m, 5H), 4.76 – 4.36 (m, 2H), 3.97 (m, 1H), 3.75-2.95 (m, 8H), [3.24 (s) and 3.19 (s), 3H], [3.19 (s) and 3.16 (s), 3H], [3.05 (s) and 2.97 (s), 3H], [2.83 (dd, J = 11.0 and 2.7 Hz,), 2.79 (dd, J = 10.7 and 3.9 Hz, 1H], 2.45-0.80 (m, 26H), [1.63 (s) and 1.61 (s), 3H], [0.77 (t, J = 7.4) and 0.76 (t, J = 7.4 Hz, 3H]; ^{13}C NMR (126 MHz, DMSO-d_6) δ 173.98, 173.84, 173.65, 173.58, 172.69, 172.61, 171.18, 171.15, 169.35, 169.07, 158.80, 158.55, 158.29, 158.03, 138.21, 137.99, 129.39, 129.14, 128.51, 126.79, 126.66, 118.46, 116.09, 113.72, 85.89, 81.90, 77.98, 77.84, 69.44, 69.39, 61.43, 60.65, 59.00, 58.66, 57.60, 57.55, 56.61, 55.98, 55.76, 53.47, 52.49, 47.56, 46.61, 44.70, 43.56, 43.38, 40.63, 40.53, 40.46, 40.37, 40.29, 40.20, 40.12, 40.04, 39.95, 39.87, 39.70, 39.53, 37.70, 36.95, 36.87, 35.87, 35.61, 32.53, 32.05, 31.73, 30.24, 30.22, 28.81, 25.71, 25.68, 24.76, 24.73, 23.58, 22.95, 22.55, 21.39, 21.37, 19.21, 19.16, 19.13, 18.91, 16.08, 15.82, 15.67, 15.61, 15.33, 14.40, 10.85, 10.63. HRMS *m/z* 730.4755 $[M + H]^+$. Calcd for $C_{39}H_{63}N_5O_8$, 730.4749.

Experimental procedure for cytotoxicity assays

N87 cells were obtained from ATCC (Manassas, VA) and were originally derived from a liver metastasis of gastric carcinoma. BT474 cells (ATCC) are derived from a breast carcinoma. MDA-MB-361-DYT2 cells are derived from breast carcinoma and were generously provided by

Dr. Dajun Yang of Georgetown University. Cells were seeded in 96-well plates at low density, then treated the following day with compounds in 3-fold serial dilutions at 10 concentrations in duplicate. Cells were incubated for 4 days in a humidified 37°C/5% CO_2 incubator. The plates were harvested by incubating with CellTiter® 96 AQueous One MTS Solution (Promega, Madison, WI) for 1.5 hour and absorbance measured on a Victor plate reader (Perkin-Elmer, Waltham, MA) at wavelength 490 nm. IC_{50} values were calculated using a four-parameter logistic model with XLfit (IDBS, Bridgewater, NJ).

ASSOCIATED CONTENT

Supporting Information

Crystallography materials and methods, determination of the absolute configuration for amino acids **19i**, **19j**, **19k** and **19l**, and NMR spectra for all new analogs are provided. This material is available free of charge via the Internet at http://pubs.acs.org.

AUTHOR INFORMATION

Corresponding Author

*E-mail: andreas.maderna@pfizer.com. Phone: 860-715 6498

Notes

The authors declare no competing financial interest. All animal experiments were performed in accordance with institutional guidelines as defined by institutional Animal Care and Use Committee for U.S. institutions.

ABBREVIATIONS

ADME, administration distribution metabolism excretion; ADC, antibody drug conjugate; MMAD, monomethyl auristatin-D; MMAE, monomethyl auristatin-E; MMAF, monomethyl auristatin-F; Dov, dolavaline; Dil, dolaisoleuine; Dap, dolaproine; Doe, dolaphenine; HATU, 1-[bis(dimethylamino)methylene]-1*H*-1,2,3-triazolo[4,5-*b*]pyridinium 3-oxid hexafluorophosphate; N-Pg, protected amine; Aib, 2-aminoisobutyric acid; GI_{50}, concentration for 50% of maximal inhibition of cell proliferation; RRCK, Ralph Russ Canine Kidney; P_{app}, apparent permeability; MDR, multi drug resistance; HLM, human liver microsome; Cl, clearance; HHEP, human liver hepatocytes; AUC, area under the concentration time curve; Vss, apparent volume of distribution; rCYP, human recombinant cytochrome P450.

REFERENCES

(1) Pettit, G. R.; Kamano, Y.; Herald, C. L.; Tuinman, A. A.; Boettner, F. E.; Kizu, H.; Schmidt, J. M.; Baczynskyj, L.; Tomer, K. B.; Bontems, R. J. The isolation and structure of a remarkable marine animal antineoplastic constituent: dolastatin 10. *J. Am. Chem. Soc.* **1987**, *109*, 6883-6885.

(2) Bai, R.; Pettit, G. R.; Hamel, E. Dolastatin 10, a powerful cytostatic peptide derived from a marine animal. Inhibition of tubulin polymerization mediated through the vinca alkaloid binding domain. *Biochem. Pharmacol.* **1990**, *39*, 1941-1949.

(3) Luesch, H.; Moore, R. E.; Paul, V. J.; Mooberry, S. L.; Corbett, T. H. Isolation of dolastatin-10 from the marine cyanobacterium Symploca species VP642 and total stereochemistry and biological evaluation of its analogue symplostatin 1. *J. Nat. Prod.* **2001**, *64*, 907-910.

(4) Harrigan, G. G.; Goetz, G. Symbiotic and dietary marine microalgae as a source of bioactive molecules-experience from natural products research. *J. Appl. Phycol.* **2002**, *14*, 103-108.

(5) Pettit, G. R.; Singh, S. B.; Hogan, F.; Lloyd-Williams, P.; Herald, D. L.; Burkett, D. D.; Clewlow, P. J. Antineoplastic agents. Part 189. The absolute configuration and synthesis of natural (-)-dolastatin-10. *J. Am. Chem. Soc.* **1989**, *111*, 5463-5465.

(6) Cormier, A.; Marchand, M.; Ravelli, R. B.; Knossow, M. Gigant, B. Structural insight into the inhibition of tubulin by vinca domain peptide ligands. *EMBO Rep.* **2008**, *9*, 1101-1106.

(7) Newman, R. A.; Fuentes, A.; Covey, J. M.; Benvenuto, J. A. Preclinical pharmacology of the natural marine product dolastatin 10 (NSC 376128). *Drug Metab. Dispos.* **1994**, *22*, 428-432.

(8) Mirsalis, J. C.; Schindler-Horvat, J.; Hill, J. R.; Tomaszewski, J. E.; Donohue, S. J.; Tyson CA. Toxicity of dolastatin 10 in mice, rats and dogs and its clinical relevance. *Cancer Chemother. Pharmacol.* **1999**, *44*, 395-402.

(9) Pitot, H. C.; McElroy, E. A. Jr.; Reid, J. M.; Windebank, A. J.; Sloan, J. A.; Erlichman, C.; Bagniewski, P. G.; Walker, D. L.; Rubin, J.; Goldberg, R. M.; Adjei, A. A.; Ames, M. M. Phase I trial of dolastatin-10 (NSC 376128) in patients with advanced solid tumors. *Clin. Cancer Res.* **1999**, *5*, 525-531.

(10) Madden, T.; Tran, H. T.; Beck, D.; Huie, R.; Newman, R. A.; Pusztai, L.; Wright, J. J.; Abbruzzese, J. L. Novel marine-derived anticancer agents: a phase I clinical, pharmacological, and pharmacodynamic study of dolastatin 10 (NSC 376128) in patients with advanced solid tumors. *Clin. Cancer Res.* **2000** , *6*, 1293-1301.

(11) Margolin, K.; Longmate, J.; Synold, T. W.; Gandara, D. R.; Weber, J.; Gonzalez, R.; Johansen, M. J.; Newman, R.; Baratta, T.; Doroshow, J. H. Dolastatin-10 in metastatic melanoma: a phase II and pharmokinetic trial of the California Cancer Consortium. *Invest*. *New Drugs* **2001**, *19*, 335-340.

(12) von Mehren, M.; Balcerzak, S. P.; Kraft, A. S.; Edmonson, J. H.; Okuno, S. H.; Davey, M.; McLaughlin, S.; Beard, M. T.; Rogatko A. Phase II trial of dolastatin-10, a novel anti-tubulin agent, in metastatic soft tissue sarcomas. *Sarcoma* **2004**, *8*, 107-111.

(13) Perez, E. A.; Hillman, D. W.; Fishkin, P.A.;, Krook, J.E.; Tan, W.W.; Kuriakose, P.A.; Alberts, S.R.; Dakhil, S.R. Phase II trial of dolastatin-10 in patients with advanced breast cancer. *Invest*. *New Drugs* **2005**, *23*, 257-261.

(14) Miyazaki, K.; Kobayashi, M.; Natsume, T.; Gondo, M.; Mikami, T.; Sakakibara, K.; Tsukagoshi, S. Synthesis and antitumor activity of novel dolastatin 10 analogs. *Chem*. *Pharm*. *Bull*. **1995**, *43*, 1706-1718.

(15) Kobayashi, M.; Natsume, T.; Tamaoki, S.; Watanabe, J.; Asano, H.; Mikami, T.; Miyasaka, K.; Miyazaki, K.; Gondo, M.; Sakakibara, K.; Tsukagoshi, S. Antitumor activity of TZT-1027, a novel dolastatin 10 derivative. *Jpn*. *J. Cancer Res*. **1997**, *88*, 316-327.

(16) Pettit, G. R.; Srirangam, J. K.; Barkoczy, J.; Williams, M. D.; Durkin, K. P.; Boyd, M. R.; Bai, R.; Hamel, E.; Schmidt, J. M.; Chapuis, J. C. Antineoplastic agents 337. Synthesis of dolastatin 10 structural modifications. *Anti-Cancer Drug Des*. **1995**, *10*, 529-544.

(17) Flahive, E.; Srirangam, J. The dolastatins. In *Anticancer agents from natural products*, 2nd ed, Cragg, D. J.; Kingston, G. M.; Newman, D. G. I., Eds., CRC Press, 2011, pp 263-290.

(18) Pettit, G. R.; Srirangam, J. K. Preparation of pentapeptides as neoplasm inhibitors. Can. Pat. Appl. CA 2114156, 1994.

(19) Pettit, G. R.; Barkoczy, J. Preparation of tumor inhibiting tetrapeptide phenethylamides. Eur. Pat. Appl. EP 600744, 1994.

(20) Doronina, S. O.; Toki, B. E.; Torgov, M. Y.; Mendelsohn, B. A.; Cerveny, C. G.; Chace, D. F.; DeBlanc, R. L.; Gearing, R. P.; Bovee, T. D.; Siegall, C. B.; Francisco, J. A.; Wahl, A. F.; Meyer D. L.; Senter, P. D. Development of potent monoclonal antibody auristatin conjugates for cancer therapy. *Nat*. *Biotechnol*. **2003**, *21*, 778-784.

(21) Senter, P. D.; Sievers, E. L. The discovery and development of brentuximab vedotin for use in relapsed Hodgkin lymphoma and systemic anaplastic large cell lymphoma. *Nat*. *Biotechnol*. **2012**, *30*, 631-637.

(22) Chari, R. V.; Miller, M. L.; Widdison, W.C. Antibody-drug conjugates: an emerging concept in cancer therapy. *Angew*. *Chem*. *Int*. *Ed*. **2014**, *53*, 3796-827.

(23) Doronina, S. O.; Mendelsohn, B. A. Preparation of auristatins having an aminobenzoic acid unit at the N terminus. PCT Int. Appl. WO 2006132670, 2006.

(24) Pettit, G. R.; Williams, M. D.; Srirangam, J. K. Preparation of dolastatin analog pentapeptide methyl esters as anticancer agents. Eur. Pat. Appl. EP 695759, 1996.

(25) Mendelsohn, B. A.; Barnscher, S. D. Preparation of substituted peptide analogs as tubulin polymerization inhibitors for treating cancers. U.S. Pat. Appl. Publ. US 20130190248, 2013.

(26) Miao, Z; Hong, Y.; Zhu, T. Preparation of drug-conjugates, particularly peptide derivative-antibody conjugates, and their uses for treating cancers. PCT Int. Appl. WO 2013173393, 2013.

(27) Gajula, P. K.; Asthana, J.; Panda, D.; Chakraborty, T. K. A synthetic dolastatin 10 analogue suppresses microtubule dynamics, inhibits cell proliferation, and induces apoptotic cell death. *J. Med. Chem.* **2013**, *56*, 2235-2245.

(28) Park, Y. J.; Jeong, J. K.; Choi, Y. M.; Lee, M. S.; Choi, J. H.; Cho, E. J.; Song, H.; Park, S. J.; Lee, J.-H.; Hong, S. S. Dolastatin-10 derivative as anticancer agent and preparation method thereof. PCT Int. Appl. WO 2014046441, 2014.

(29) Harrigan, G. G.; Luesch, H.; Yoshida, W. Y.; Moore, R. E.; Nagle, D. G.; Paul, V. J.; Mooberry, S. L.; Corbett, T. H.; Valeriote, F. A. Symplostatin 1: a dolastatin 10 analogue from the marine cyanobacterium symploca hydnoides. *J. Nat. Prod.* **1998**, *61*, 1075-1077.

(30) Hamada, Y.; Hayashi, K.; Shioiri, T. Efficient stereoselective synthesis of dolastatin 10, an antineoplastic peptide from a sea hare. *Tetrahedron Lett.* **1991**, *32*, 931-934.

(31) Mordant, C.; Reymond, S.; Tone, H.; Lavergne, D.; Touati, R.; Ben Hassine, B.; Ratovelomanana-Vidal, V.; Genet, J. P. Total synthesis of dolastatin 10 through ruthenium-catalyzed asymmetric hydrogenations. *Tetrahedron*, **2007**, *63*, 6115-6123, and references therein.

(32) Kline, T.; Torgov, M. Y.; Mendelsohn, B. A; Cerveny, C. G.; Senter, P. D. Novel antitumor prodrugs designed for activation by matrix metalloproteinases-2 and -9. *Mol Pharmaceutics* **2004**, *1*, 9-22.

(33) Venkatraman, J.; Shankaramma, S. C.; Balaram, P. Design of Folded Peptides. *Chem. Rev.* **2001**, *101*, 3131-3152.

(34) Mukhtar, E.; Adhami, V.M.; Mukhtar, H. Targeting microtubules by natural agents for cancer therapy. *Mol*. *Cancer Ther*. **2014**, *13*, 275-284.

(35) Di, L.; Whitney-Pickett, C.; Umland, J. P.; Zhang, H.; Zhang, X.; Gebhard, D. F.; Lai, Y.; Federico, J. J. 3rd.; Davidson, R. E.; Smith, R.; Reyner, E. L.; Lee, C.; Feng, B.; Rotter, C.; Varma, M. V.; Kempshall, S.; Fenner, K.; El-Kattan, A. F.; Liston, T. E.; Troutman, M. D. Development of a new permeability assay using low-efflux MDCKII cells. *J*. *Pharm*. *Sci*. **2011**, *100*, 4974-4985.

(36) Gigant, B.; Curmi, P. A.; Martin-Barbey, C.; Charbaut, E.; Lachkar, S.; Lebeau, L.; Siavoshian, S.; Sobel, A.; Knossow, M. The 4A X-ray structure of a tubulin:stathmin-like domain complex. *Cell* **2000**, *102*, 809-816.

(37) Ranaivoson, F. M.; Gigant, B.; Berritt, S.; Joullié, M.; Knossow, M. Structural plasticity of tubulin assembly probed by vinca-domain ligands. *Acta Crystallogr*., *Sect*. *D*: *Biol*. *Crystallogr*. **2012**, *8*, 927-934.

(38) Nawrotek, A.; Knossow, M.; Gigant, B. The determinants that govern microtubule assembly from the atomic structure of GTP-tubulin. *J*. *Mol*. *Biol*. **2011**, *412*, 35-42.

(39) Kang, Y. K.; Park, H. S. Internal rotation about the C–N bond of amides. *J. Mol. Struct.: THEOCHEM* **2004**, *676*, 171–176.

(40) Alattia, T.; Roux, F.; Poncet, J.; Cave, A.; Jouin, P. Conformational study of dolastatin 10. Tetrahedron **1995**, *51*, 2593-2604.

(41) Benedetti, E.; Carlomagno, T.; Fraternali, F.; Hamada, Y.; Hayashi, K.; Paolillo, L.; Shioiri, T. Conformational analysis of dolastatin 10: an NMR and theoretical approach. *Biopolymers* **1995**, *35*, 525-538.

(42) Pettit, G. R.; Sirangam, J. K.; Herald, D. L.; Hamel, E. J. The Dolastatins. 21. Synthesis, X-ray crystal structure, and molecular modeling of (6*R*)-isodolastatin 10. *J. Org. Chem*. **1994**, *59*, 6127-6130.

(43) Pauletti, G. M.; Gangwar, S.; Siahaan, T. J.; Aube, J.; Borchardt, R. T. Improvement of oral peptide bioavailability: Peptidomimetics and prodrug strategies. *Adv. Drug Delivery Rev.* **1997**, *27*, 235-256.

(44) Obach, S. Prediction of human clearance of twenty-nine drugs from hepatic microsomal intrinsic clearance data: an examination of in vitro half-life approach and nonspecific binding to microsomes. *Drug Metab*. *Dispos*. **1999**, *27*, 1350-1359.

(45) Han, T. H.; Gopal, A. K.; Ramchandren, R.; Goy, A.; Chen, R.; Matous, J. V.; Cooper, M.; Grove, L. E.; Alley, S. C.; Lynch, C. M.; O'Connor, O. A. CYP3A-mediated drug-drug interaction potential and excretion of brentuximab vedotin, an antibody-drug conjugate, in patients with CD30-positive hematologic malignancies. *J. Clin*. *Pharmacol*. **2013**, *53*, 866-877.

(46) Hirth, J.-A.; Watkins, P. B.; Strawderman, M.; Schott, A.; Bruno, R.; Baker, L. H. The effect of an individual's cytochrome CYP3A4 activity on docetaxel clearance. *Clin Cancer Res*. **2000**, *6*, 1255-1258.

(47) Doroski, M. D.; Maderna, A.; O'Donnell, C. J.; Subramanyam, C.; Vetelino, B. C.; Dushin, R. G.; Strop, P.; Graziani, E. I. Preparation of cytotoxic pentapeptides and their antibody drug conjugates for treating cancer. PCT Int. Appl. WO 2013072813, 2013.

(48) Pettit, G. R.; Barkoczy, J.; Srirangam, J. K.; Singh, S. B.; Herald, D. L.; Williams, M. D.; Kantoci, D.; Hogan, F.; Groy, T. L. The Dolastatins. 22. Synthesis of Boc-dolaproinyl-dolaphenine and four related chiral isomers. *J. Org. Chem.* **1994**, *59*, 2935-2938.

Table of Contents graphic

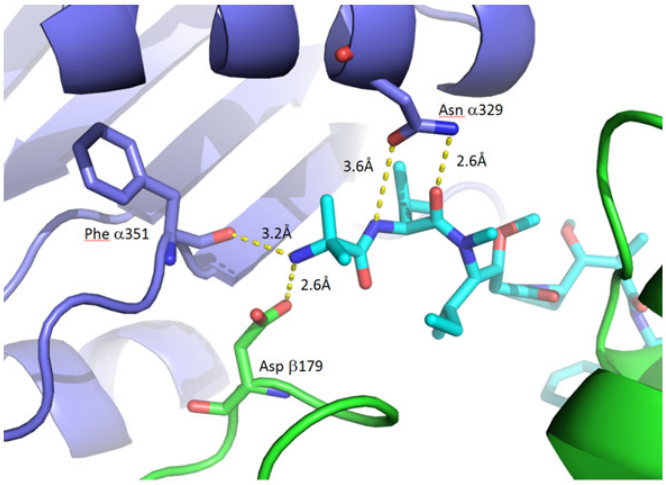

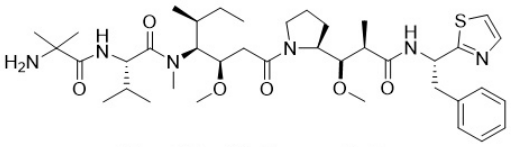

GI_{50}: 0.2 nM Cancer Cells